Robotica (2023), **41**, pp. 2365–2396
doi:10.1017/S0263574723000449

CAMBRIDGE UNIVERSITY PRESS

RESEARCH ARTICLE

Design, modeling, and manufacturing of a novel robust gripper-based climbing robot: KharazmBot

Vahid Boomeri, Hami Tourajizadeh, Hamid Reza Askarian and Sina Pourebrahim

Faculty of Engineering, Kharazmi University, Tehran, Iran
Corresponding author. Hami Tourajizadeh; Email: Tourajizadeh@khu.ac.ir

Received: 18 June 2022; **Revised:** 5 March 2023; **Accepted:** 24 March 2023; **First published online:** 11 May 2023

Keywords: climbing robot, prototype manufacturing, grip-based locomotion, hybrid mechanism, robust gripper

Abstract

There are a lot of high-height structures that should be inspected or manipulated frequently due to maintenance purposes. According to the safety considerations and time or cost limitations, substituting the human operator with an automatic robot is inevitable. The main objective of this paper is to design and manufacture a novel climbing robot equipped with grip-based locomotion system which can climb through scaffold structures and trusses to accomplish inspectional and operational tasks. The proposed robot has good maneuverability and stability. The proposed robot is manufactured in order to verify the simulation results with experimental data. The chassis and its corresponding grippers are designed first, and the corresponding model of the system is extracted. This model is used then for designing the controlling strategy of the system. The path planning of the robot is conducted to realize the climbing process by the robot during several steps in an optimum way. The prototype of the proposed robot is manufactured at Kharazmi University called KharazmBot. Experimental results not only show the capability of the manufactured robot toward ascending the mentioned structures but also prove its high stability as a result of its designed gripper and also its good maneuverability as a result of its over-actuated mechanism. Thus, it is concluded that the designed and manufactured climbing robot of this paper can successfully ascend through the pipes and trusses and perform a desired inspectional or operational task with good accuracy and safety while its stability is also satisfied.

1. Introduction

Inspection and manipulation of industrial installations are extremely difficult and costly for repair and maintenance organizations. Recently through the promotion of automatic and smart technologies, vast types of robots are designed and proposed to accomplish the mentioned inspectional and operational tasks. The first generation of these kinds of robots was based on mobile robots by which the chassis of the manipulator can travel to the target zone on a flat surface to perform the desired mission. However, each environment needs its special locomotion system such that the robot could be able to move through. As a result, different kinds of mobile robots capable of traveling through the air, water, etc. have been proposed so far, and their related design, modeling, and control are studied. A novel case of inspection robot which needs special consideration is the one that is responsible for climbing through some special structures such as trusses in order to inspect or manipulate at high heights. Climbing robots are the kinds of moving robots that can overcome the gravity of the earth and ascend from a target structure. The usage of climbing robots has grown intensively in recent decades. These robots are significantly important from the safety point of view since the danger of the operator falling can be neutralized by the aid of these robots. Different kinds of climbing robots are proposed and manufactured so far each of which has special capabilities and can ascend through special structures. Therefore, depending on the used locomotion mechanism, climbing robots should be designed according to their special tasks. However, most of the known climbing robots move using wheels or adhesive cups and can climb through flat surfaces like walls and windows. Because there are a lot of scaffold structures on which the operators

have to work, the importance of designing and proposing a climbing robot with a grip-based locomotion mechanism to ascend the truss-shaped structures can be sensed. The most important challenge in designing such climbing robots is providing a compromise among the speed, stability, and precision since the robot is supposed to ascend against gravity through the pipe-shaped frames. Falling hazards and mortality rates as the result of working at high heights for workers form 25% of the death statistics related to construction sites [1]. This dramatic statistic is significantly reduced recently thanks to the development of ascending robots that are able to climb through pipe-framed structures, metallic bridges, astronomy equipment, scaffolds, trusses, etc. Regular access to structures like oil and gas refineries, aerospace industries, electric power transmission maintenance, telecommunication towers, construction of sports and recreational salons for periodic inspections, and continuous yearly and monthly maintenance are some examples for which climbing through them requires a high financial cost and results in corporeal damages. These casualties can be eliminated using the proposed climbing robots. As a result, special robots with innovative locomotion mechanisms are required to fulfill the mentioned target for climbing through the infrastructures. It is desired to design and manufacture the climbing robot with the least amount of cost and the best stability conditions which could be able to perform operations such as welding, construction, inspection, etc.

Some previous research has studied the modeling, control, or manufacturing of these kinds of robots. In ref. [2], the categorization of climbing robots is discussed according to their functionality and duties. Stoeter & Papanikolopoulos [3] proposed a stair-climbing robot. However, this robot cannot ascent through the trusses. CMR (compliant modular robot) [4] is an example of a modular wheeled robot that can tackle the overhangs to climb over the stairs. For ascending walls or flat terrains, adhesive robots can be employed known as wall-climbing robots. ROMA II [5] is an example of such climbing robots in which the direct and inverse kinematics of this robot is investigated. Another robot that is equipped with a suction pump is W-Climbot [6] designed for climbing walls. The analysis of equilibrium is investigated by calculating the friction forces related to the suction grippers to avoid falling incidents due to the gravity force. There are also some climbing robots equipped with wheels that can move over walls or even straight poles. A human-inspired climbing robot for ascending the poles for periodic services is proposed in ref. [7]. Here, the proposed robot is based on a self-stable concept in which the static and stability analysis is calculated and simulated by MSC-ADAMS to ensure the falling avoidance. The wheel-based robots can also be inspired by animals especially insects which are known as bionic robots. In ref. [8], the wheels are spine wheels that can stick to the concrete walls with tiny claws and adhesive suction forces on the wheels as they rotate. As explained previously, the climbing robots are not limited to flat surfaces like walls, etc. There is another generation of climbing robots that can climb over the poles and straight or curved pipes. In PCR [9], Stewart mechanism is employed with the ability of climbing through the curved ducts that can maneuver through the branches of duct frames with both tubular and rectangular cross-section profiles. For cable climbing robot, in ref. [10] a robot is introduced which can grasp the circular cross-section structures like cables. This robot can be used for cable maintenance and reparing operation like grinding, painting, crack inspections of the surfaces related to the pipes or tube-shaped objects. The critical behavior of the robot dynamics is simulated in MSC-ADAMS, and for the experiment, a simple double-loop PD controller is designed to track the commanded path based on the inverse kinematics and the feedback of the sensors.

However, the mentioned climbing robots are not able to ascend through the frame-shaped structures. ROMA I [11] is a limbed climbing robot with 8 DOFs that can ascend through the infrastructures and metallic bridges for repair and maintenance purposes. This robot can move over metallic beams for construction activities. The locomotion of the ROMA is provided by the designed GUI in which the algorithm of moving is predefined. An adaptive pole climbing robot is proposed in ref. [12] that can move in two modes called ground crawling and pole climbing. By reducing the driving sources, stability and self-adaptivity are realized. Another robot that can perform inspections and implement fastening and welding tasks over 3D pipe-shaped structures is 3D-CLIMBER [13] which can grasp the pipes with its grasping mechanism to travel through the frame. A serial manipulator is installed on the robot to perform manipulative tasks. The locomotion of this 4-DOFs robot is performed according to the inverse

https://doi.org/10.1017/S0263574723000449 Published online by Cambridge University Press

and forward kinematics used for designing the motion algorithm. For this case, a GUI control panel is designed to command the robot's motion. For climbing over the pipes and rods, some flexible robots can be used like SR-CR [14] which is presented as a soft rod climbing robot with four flexible arms that can bend easily to grasp the aimed rods by the power of pneumatic source and actuators. Another example of flexible robots which can climb over rods and pipes is a Spine robot [15] which can move like a caterpillar with its tiny claws over the poles, etc. and is grouped as the Bionic robot. Another bionic robot inspired by animals and insects is an inch-worm climbing robot proposed in ref. [16] in which the kinematics and dynamics modeling of the robot is extracted by the screw theory. Shady3D [17] is a modular robot for ascending through the trusses in which the modules of the robot can attach together or detach to perform moving procedures over the truss-shaped profiles. Damped least square method is used for the approximation algorithm based on the manipulator Jacobean instead of the explicit solution. Climbot [18] is a serial robot that can climb over straight electrical poles or even move over 3D trusses with computer vision utilities. Here path planning can be achieved by recognizing the truss structure by the installed cameras on the robot. The whole locomotion of the robot is divided into finite gates or steps. The forward kinematics of this 5 DOFs robot is calculated by Denavit-Hartenberg parameters. Dynamic calculation of a legged climbing-walking robot is extracted in ref. [19] with details including the dynamic modeling of the robot's locomotion using gait planning of motions. To travel over 2D frames, Libra [20] is designed which consists of the main body and three limbs attached by revolute joints in order to climb through the truss-shaped frames related to the space industry such as huge space satellites. Action module methodology is performed for experimental tests of the robot climbing beside the genetic algorithm for ascending the test beds with special patterns. Also for space services and maintenances, a specific robot is introduced and discussed named Chameleon-like robot [21] with three arms and three grippers that are used for the robot to grasp the piped structures and move over them to carry out special tasks in space stations like assembling, repairing monitoring, and etc. However, the grippers are weak, and also since no prismatic joint is employed, its translational workspace of the chassis is more limited.

Most of the mentioned climbing robots for ascending through the infrastructures are grip-based robots that can also pass the obstacles. These robots have great maneuverability and stability. Hence, for a climbing robot that is supposed to travel through the scaffolds or pipe-shaped frames, the related grippers should be also investigated. In ref. [22], many gripping or grasping robots and mechanisms are reviewed based on the different techniques and mechanisms from robust gripping to soft and precise grasping. The concept of design strategies for proper grippers is discussed in detail in ref. [23] in which the characteristics of a grasping operation are introduced. Self-locking under-actuated mechanism [24] is an under-actuated gripper with three fingers and two DOFs. One DOF is for moving the fingers, and the other one is related to locking the gripper. This gripper can grasp various kinds of objects with different shapes. The static analysis is performed using the contact forces of the fingers and their related moments. Another under-actuated gripper which is equipped with two fingers is introduced in ref. [25] for which each finger is driven by an actuator. The fingers are formed by two links connected together by a revolute joint to grasp the objects with different shapes. This gripper has the locking capability during grasping moments to avoid the back drivability phenomenon. The tendon-driven bio-inspired robotic hand is another example of a robotic hand for dexterous manipulations just like the real hands. In ref. [26], a tendon-based transmission system is investigated and designed, and LMS (Laboratoire de Mécanique des Solides) limitations are solved and modified. LARM [27] is an example of a gripper inspired by the human hand which has three fingers while each finger is driven by a rotary actuator to grasp the spherical and cylindrical objects. In ref. [28], grasping the objects with different geometrical shapes by the multi-fingers strategy is studied and modeled to derive the computer command code for grasping the objects precisely despite their unknown shapes. Grasping operations for hand grippers are also investigated in ref. [29]. The related strategies for different kinds of grasping process are studied here in order to design a proper hand mechanism for a multi-fingered under-actuated gripper. By using the Scott-Russel mechanism, a gecko-like gripper can be designed and an adhesive form of the grasping

https://doi.org/10.1017/S0263574723000449 Published online by Cambridge University Press

of this gripper is presented in ref. [30]. The modeling of the adhesive friction is illustrated here for grasping the objects and holding them. Some grippers are specially designed and manufactured for climbing purposes. For example, a new kind of gripper is proposed in ref. [31] to apply for climbing robots. The gripper has a v-shaped mechanism driven by an actuator using worm gear in order to avoid the back drivability phenomenon and provide robust grasping. The static analysis is performed in this work to ensure the gripper stability using the friction forces of the fingers. For claw grasping robots which ascend through the walls, in order to meet the stable situation considering the friction coefficient, ref. [32] has extracted a mathematical relation between the angle of the hook and the coefficient of friction in which the condition of self-lock related to friction occurs.

As can be seen, a proper mechanism is not presented yet by which the climbing through the pipe-frames and scaffold structures could be realized with good stability and maneuverability. In order to cover the mentioned target, a redundant hybrid mechanism is designed and modeled in this paper according to a grip-based locomotion system that is inspired by the monkeys' movement through the trees or gymnastic athletes moving through the barfix bars. Since two supporting limbs are always engaged, the robot is self-stable, and the stability of the system can be guaranteed while the third limb provides the maneuverability of the robot. Thus, the biped grip-based mechanism is a proper choice for ascending the aimed targets. These kinds of robots are known as brachiation robots which are inspired mostly by armed animals like apes and sloths. A survey on this category of robots with dynamics and control schemes is introduced in ref. [33]. Also, the sustainability of this robot is increased as a result of using the legs in the robot. Therefore, the proposed robot is able to ascend the trusses and infrastructures with different patterns. Besides, a biped grip-based mechanism is a proper choice for carrying loads through the pipes and bars. Thus, the robot can tolerate high payloads against the gravity as a result of its special design. Also, a novel gripper is presented here, capable of realizing climbing with an exceptional degree of grasping strength and a locking feature that can tolerate the whole robot's weight with the least amount of slippage possibility. Since the grippers are locked by locking pliers, the robot has enough stability to perform operational tasks. Furthermore, as a result of the redundant mechanism of the designed robot, not only the possibility of energy saving is provided by proper actuating switching but also the maneuverability of the robot is extremely increased resulting to provide the possibility of path planning and optimization purposes. This robot then can be used in scaffolds of civil infrastructures for elevating materials and equipment. It can perform operational tasks such as welding and grinding over the height. It can also be employed in some pipeline installations for inspecting the installations and performing maintenance. In all of the mentioned items, the danger of death and falling the operator can be eliminated. The prototype of the designed robot is also manufactured in the Kharazmi University called KharazmBot, and the mentioned claims are verified by conducting some experimental tests on this system. Thus, the novelty of the paper is to design, modeling, and manufacturing a prototype of a new robot consisting of proper mechanisms which could be capable of moving and climbing through the scaffold structures without the necessity of employing a human operator in order to decrease the risk of falling and its related subsequences such as injuries or death. The existing robots cannot move within such structures.

The paper is organized as follows: the proper mechanism is designed and analyzed in the next section which can meet the mentioned expectancies. Afterward, in section three, the robot is modeled and a proper controlling strategy is designed for the planned path of the locomotion phase of the robot. Section four describes the manufacturing process of the robot including its mechanical part assembling, providing its electronic equipment such as actuators, sensors, and data transfer protocol, implementing the controlling strategy, and providing a proper GUI for the operator. Afterward, in section five, the required tests are conducted and the efficiency of the proposed robot toward ascending the structures is verified by analyzing the experimental data. It is proved that with the aid of the designed and manufactured novel climbing robot and its related grippers, it is possible to ascend through all kinds of 2D infrastructures in which the pipes are perpendicular to the plane of motion. The robot can climb by a series of motions and implement any inspectional and manipulating operations successfully in a safe and low-risk condition.

https://doi.org/10.1017/S0263574723000449 Published online by Cambridge University Press

2. Robot design

2.1. Moving chassis

As explained in the introduction section, the designed robot should have good stability and maneuverability during its climbing through the structures so that it could be able to take the required equipment from the ground to the desired height and also perform related operations such as welding, maintenance, inspection, etc. The movement of the robot is inspired by the monkey's motion through the trees. At any moment, the monkey takes two branches with his legs and tail simultaneously and swings using the other hand to grasp the new branch. Afterward, he releases his tail or leg to grasp a new point as a support point, and thus, the monkey movement will be performed by iterating these operations sequentially among the tree branches. Hence, in order to increase the robot's maneuverability, the biped mechanism is selected for its locomotion system which is equipped with strong grippers. Therefore, the configuration of the proposed climbing robot is a robot with three limbs that are connected to the main chassis, and its related grippers are attached to the limbs. Actually, two points are always grasped by the grippers of the limbs and are locked to the frame while the last limb is free to move. Thus, at each moment, there are two supports for the robot that provides the stability of the system while the force distribution is also properly balanced on the branches. On the other words, since this hybrid robot is a kind of parallel robot in each movement interval, the robot is suspended through at least two legs in each step of the robot movement, and thus, the stress concentration will be avoided as the result of the robot weight, and the weight force will be distributed within the engaged legs. The roles of the limbs change periodically. When the third limb grasps the target pipe, one of the locked limbs releases and again searches for a new target point on another pipe. By iterating the mentioned sequence of operations, the climbing of the robot can be realized through the pipeline structures in a planar workspace.

Figure 1 shows the KharazmBot CAD design and clarifies the configuration of the proposed climbing robot during its stand on the pipeline structure. Each limb consists of two rotational joints and a prismatic joint. The rotational joint is the connection between the limb and the triangular chassis (the shoulder joint) while the other revolute joint is the connection between the gripper and the limb (the wrist joint). The prismatic joint between these two revolute joints is a linear jack that configures the arm body of the limb. It should be noticed that during the stand of the robot on the structure with two locked limbs, not only the free limb can move but also the main chassis of the robot can have motion since the robot has a hybrid structure and the chassis forms a parallel mechanism. Therefore, we can define two sub-mechanisms consisting of parallel and serial ones. The first sub-mechanism includes the robot's triangular chassis and two limbs that are fixed on the pipe, and the second sub-mechanism is the free limb, looking for a new point to grasp. The parallel portion of the robot increases the robot's precision and stiffness and makes the robot resistant to gravity forces and instability conditions. As a matter of fact, the sustainability of the robot is provided by the aid of the robot's parallel sub-mechanism besides its firm grippers.

The mentioned climbing process is illustrated in Fig. 2.

To determine the parallel sub-mechanism mobility, its DOF (Degree of Freedom) should be calculated. To calculate the DOF of the Parallel Sub-Mechanism (PSM), Grubler's formula is employed as Eq. (1):

$$\text{PSM\_}N_{\text{DOF}} = N_w \times (N_m - N_j) + N_j \times \text{dof}_j \tag{1}$$

From Eq. (1), N_w is the number of the workspace DOF which is $N_w = 3$ for the planar workspace and Nm is the number of moving bodies which is $N_m = 5$ for this PSM. One of the moving bodies is the triangular chassis, and the rest are related to the two limbs each of which consists of two moving members, that is, jack's cylinder and piston. N_j is the number of joints of the PSM. Two revolute joints connect the grippers to the limbs (wrist joints), and the other two revolute joints connect the two limbs to the chassis (shoulder joints). Also, there are two prismatic joints for the two limbs, and thus, one can conclude that $N_j = 6$. dof_j is the number of each joint DOF which is 1 for each joint of the mentioned joints. As a result, by a simple arithmetic calculation, one can conclude that the parallel sub-mechanism is a 3 DOF system. Therefore, by actuating these three DOFs of PSM, the triangular chassis can move in a 2D workspace

https://doi.org/10.1017/S0263574723000449 Published online by Cambridge University Press

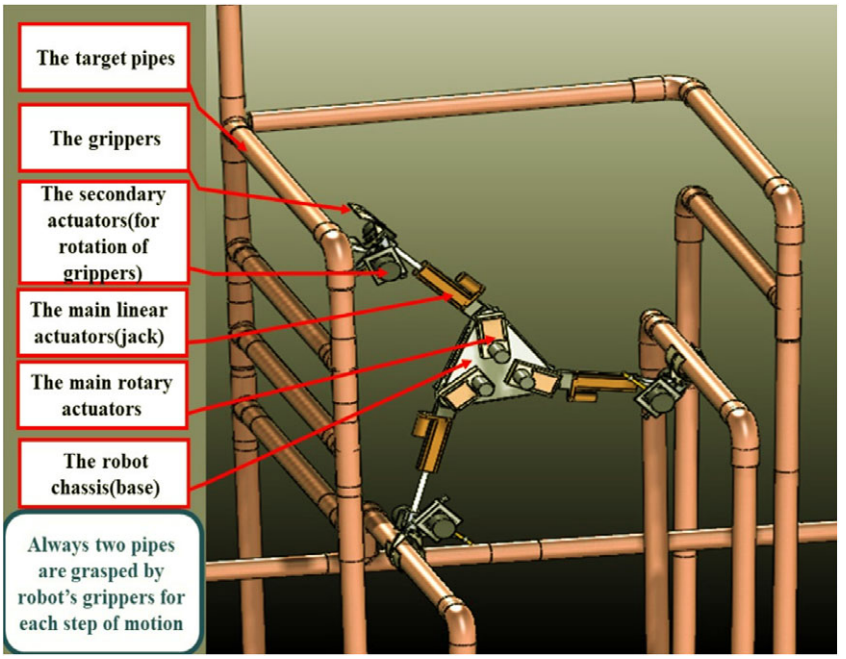

Figure 1. *The CAD design of the KharazmBot positioned on a pipeline frame.*

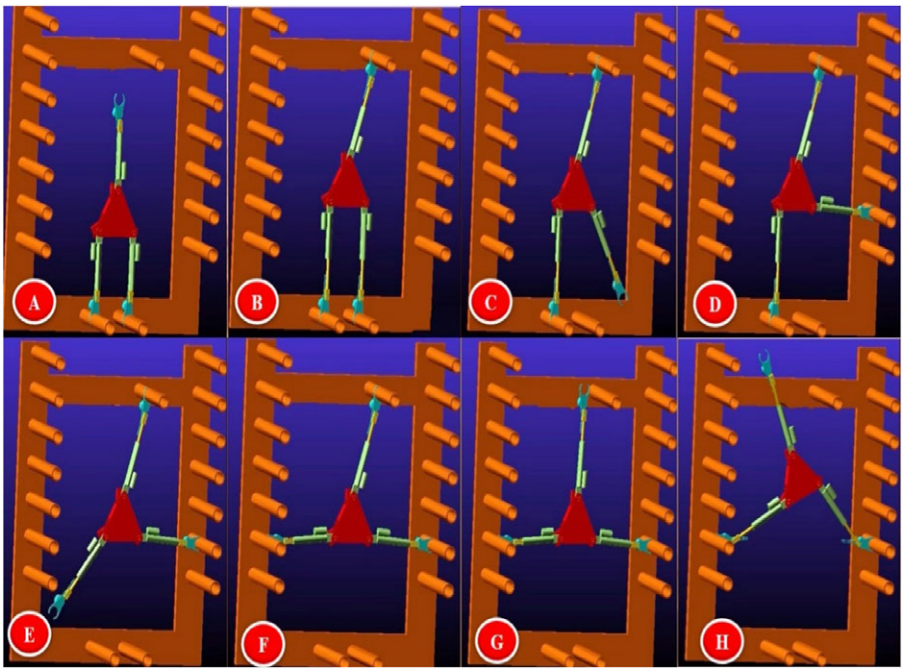

Figure 2. *The locomotion procedure of the KharazmBot.*

since the number of the system DOF and the workspace DOF are equal (PSM_$N_{\mathrm{DOF}} = N_w = 3$). Thus, the complete 2D motion of the chassis can be fulfilled by the motion of these three main joints of the PSM. The motion of the chassis in its 2D workspace caused by PSM's main joints is illustrated in Fig. 3.

As a result, the triangular chassis can move along X and Y directions and can also rotate about Z-axis which is an additive motion for the free arm. The third limb is a two DOFs serial sub-mechanism

https://doi.org/10.1017/S0263574723000449 Published online by Cambridge University Press

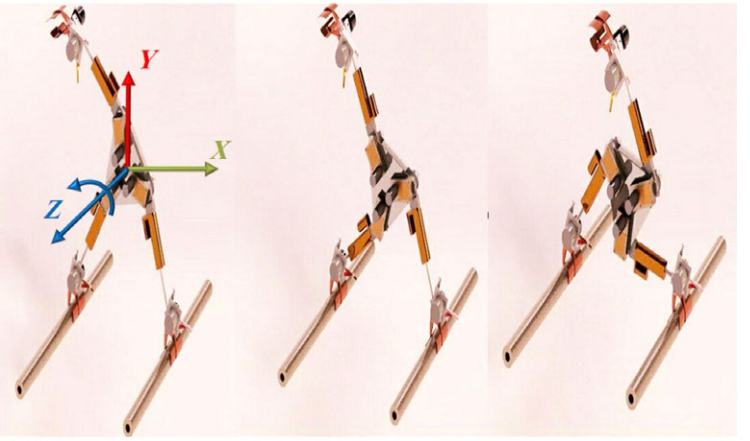

Figure 3. *The PSM motion.*

(SSM). The SSM main joints consist of a rotational joint (the shoulder joint) and one prismatic joint while the wrist joint in the free arm should not be counted as the main DOF since it is related to the gripper. According to the mentioned explanations, the combination of the three DOFs of the PSM and the two DOFs of the SSM configures the whole robot with five DOFs (Robot_$N_{\mathrm{DOF}} = 5$) by which the whole robot can move in a planar workspace. Thus, it can be concluded that the designed robot is a redundant system since the number of the robot's DOFs is greater than the planar workspace DOFs (Robot_$N_{\mathrm{DOF}} > N_w$). This fact increases the mobility of the system. In this situation, the possible paths which can be generated between two boundary conditions are not unique and the optimum solution can be obtained for the robot movement. This feature will be explained in the kinematics section in more detail. Thus since the robot is over-actuated (with redundant DOFs), it is possible to move the robot through different paths, and thus, it is possible to select the path which covers the constraints of the structure.

It should be also noticed that since the robot in its current form is not autonomous two approaches are possible for its movement. The former one is related to the structures for which, whole the workspace is observable by the operator, and thus, the operator can distinguish the next target pipe for the robot gripper according to the instantaneous location of the robot together with the observed structure. Here just a webcam needs to be installed on the gripper through which the operator can adjust the gripper position during the grasping process with respect to the pipe by checking the situation in the related monitor. Another approach which is necessary for big constructions in which whole the structure cannot be covered by the operator's eyes is offline path planning of the robot. In this case, the instantaneous location of the robot needs to be reported on a schematic plan of the structure, and the operator has to move the robot legs through the predefined path of the robot with the aid of the related map. Here again, the grasping process should be accomplished with the aid of an installed webcam on the robot legs which shows the situation of the gripper with respect to the pipes through a monitor.

2.2. The grippers

The locomotion mechanism of the proposed climbing robot is based on grippers. The grippers should be robust enough to tolerate the robot's weight and provide the robot stability. The robustness of the grippers is the key point of design since the whole robot's weight and the main motor reactions should be compensated by the aid of the grippers. To keep the robot at its desired height and avoid the robot from falling, a two-finger mechanism for the gripper structure is practically enough. The only main challenge is to avoid the slippage of the gripper with respect to the pipes. To meet this goal, the locking plier mechanism is employed here for implementing the grasping operation by which the robustness of

https://doi.org/10.1017/S0263574723000449 Published online by Cambridge University Press

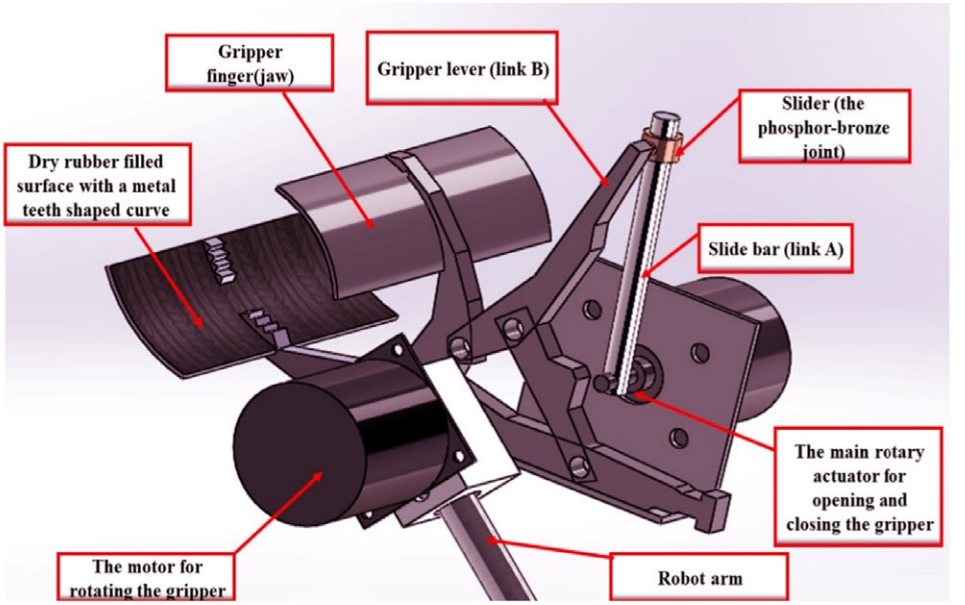

Figure 4. *The CAD model of the designed gripper with its components.*

locking can be guaranteed. Since the locking process in this mechanism is conducted using a mechanical process rather than the electrical one, it can be proved that the locking condition cannot be lost since its switch would be triggered. This is contributed to the fact that, by the aid of the designed four-bar linkage mechanism, a mechanical singularity can be realized. This means that the mechanism can be locked with little force and can be also unlocked by a toggle. The locking force is independent of energy and this force is only dependent on the strength of the related material. Hence, the mechanism would be robust enough against the falling and instability. Thus, the transmission ratio is position-dependent which causes a kind of locking singularity situation. An infinite transfer ratio means that the required torque for starting the rotation is infinite. Therefore, in this singular situation, unlocking the jaw is impossible by external disturbances [34, 35]. This locking mechanism is previously used for a walking robot as a knee lock for Dribble [36]. In this robot, the transmission ratio between the actuator and the knee is very high in singular position so with a less amount of energy, the walking robot is locked and remains stable. Here in this paper, the same singularity situation happens for the proposed mechanism which is based on locking pliers. In ref. [37], the kinetic of this plier is completely analyzed. An auxiliary mechanism is designed and added here to the locking plier to accomplish its opening and closing procedure automatically. The statics and kinematics of the proposed gripper are fully explained in ref. [38] by the same authors in which complete analysis of the locking procedure is illustrated in detail. The proposed gripper mechanism is illustrated in Fig. 4.

To demonstrate the procedure of grasping operation, a schematic view of the proposed locking mechanism is shown in Fig. 5.

From the schematic view of the designed gripper mechanism, it can be seen that the mechanism consists of two sub-mechanisms. Each mechanism is a four-bar linkage "loop1" and "loop2" which are connected to each other by a common link "b1" with revolute joints J4 and J3. In loop1, one link can be interpreted as a variable-length link that is presented as a slider bar according to the CAD view of Fig. 4. Here the slider bar and its related slider are shown by a prismatic joint (J7). The links b1, b2, d1, d2, and c are the moving members ($N_m = 5$), and there are six revolute joints with one prismatic one, ($N_j = 6$ and $\text{dof}_j = 1$). Thus considering the fact that the mechanism has a 2D planar workspace ($N_w = 3$), one can conclude according to the Grublers formula introduced in Eq. (1) that the number of DOF of the proposed gripper is 1 which can open and close the gripper's jaw by the aid of a rotary actuator. A slider

https://doi.org/10.1017/S0263574723000449 Published online by Cambridge University Press

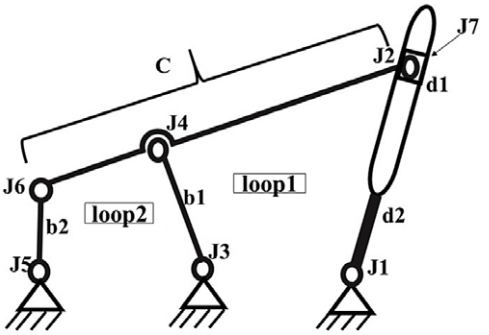

Figure 5. *The schematic view of the locking mechanism as the robot's gripper.*

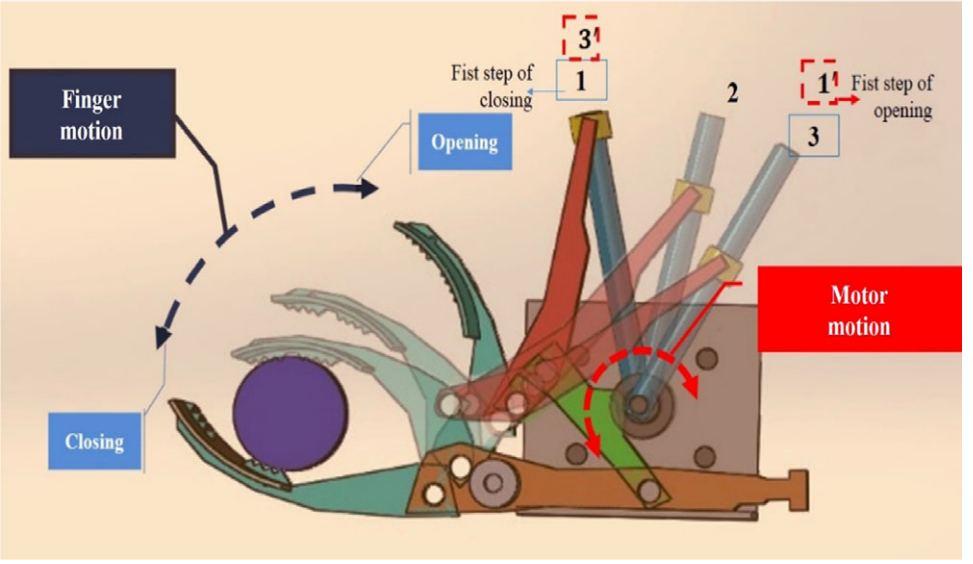

Figure 6. *The opening and closing procedure of the gripper.*

bar is connected to an actuator which can be rotated by a motor, and a slider connects the gripper lever to the slider bar. If the slider bar rotates clockwise, the gripper closes, and if the slider bar rotates counter-clockwise, the gripper opens. The motion of the gripper for implementing the open/close operation is clarified in Fig. 6.

About the stability of the proposed system, it can be analyzed from two points of view consisting of controlling stability and mechanical stability of the mechanism. About the former case, the employed controlling strategy which is PD and is studied in Section 4.2 is covered since the gains are selected by pole placement method with negative real values for the related poles. Also, the accuracy of the robot as a result of its designed controller is studied in the Section 5. However about the latter case, it should be considered that the proposed robot is essentially a parallel system which has a high stiffness. Also, the main actuators which are installed on the base chassis as stated in Section 4 are not back-drivable as a result of their high gear ratio which is about 450. Moreover, the employed jacks are based on screw without ball or bullet which makes them a kind of power transmission screw. Consequently, the stiffness of the system even in the absence of the electricity power is high enough to avoid the system of being deviated as a result of its weight. Finally, the employed grasping mechanism which is locking pliers is the best choice to guarantee the stability of the grippers since it is provable that at the locking stage, the locking plier as mentioned cannot rotate around the pipes. Here with the aid of the proposed mechanism of controlling the pliers, it can be assured that the locking stage is realized. This is contributed to the

https://doi.org/10.1017/S0263574723000449 Published online by Cambridge University Press

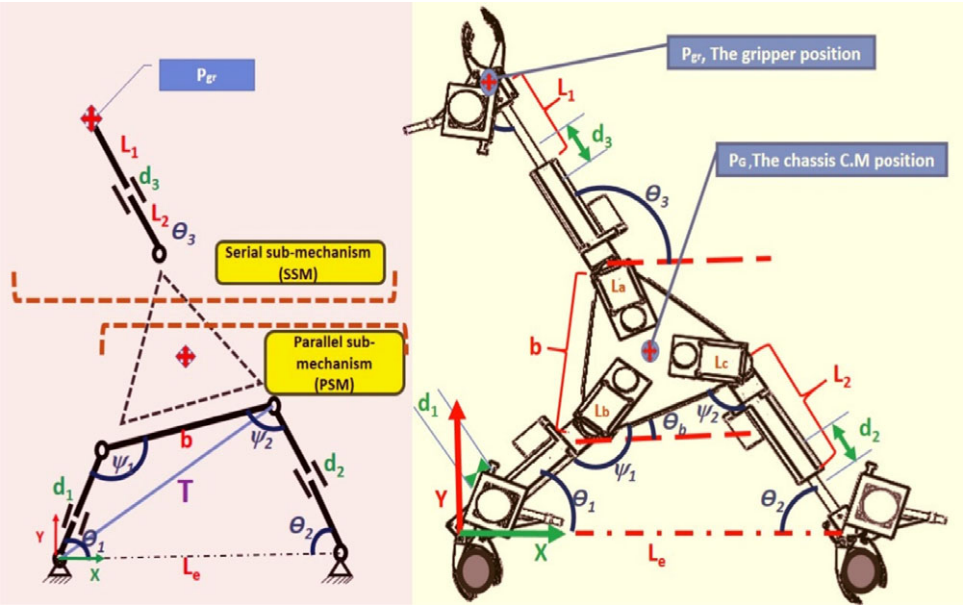

Figure 7. *The schematic view of KharazmBot for geometric clarification.*

fact that the related actuating motor rotated the corresponding mechanism link as long as the rotation is possible.

Thus, it can be concluded that the stability of the system is extremely high while the speed of the robot is low, respectively, as a result of the mentioned high gear ratios. Finally, it is notable that the diameter of the gripper which is a kind of locking plier is adjustable for different pipes with various diameters using an adjustment screw.

3. Kinematics

In this section, the kinematics of the KharazmBot is extracted. Kinematics needs to be extracted in order to control the robot and establish the relation between the workspace of the robot and its corresponding joint space. Consider the PSM which consists of six joints. At each time, just three joints are active which are the main DOFs of the PSM, and the other ones are passive. In order to extract the kinematics of the robot, we must first obtain the geometric constraints between these six joints. By extracting the geometric constraints of PSM, the functionality of all of the joints can be determined in terms of the main joints' motions. On the other side, all of the joints of the SSM which is the robot's free limb are the independent generalized coordinates of the system without any constraints, and thus, each joint of the free limb is the main DOF. In Fig. 7, the lengths of the cylinders are L_1 and the lengths of their related pistons are L_2. Also, the elongations of the jacks are shown by d_i in which i denotes the number of the jack. Joints d_1, d_2, and ψ_1 are selected as the main DOFs of the PSM by which the amount of rotational or linear displacement can be defined. Also, the joints θ_3 and d_3 are the main DOFs of the SSM in which the θ_3 declares the amount of free arm rotation and d_3 declares the amount of linear displacement of the free arm.

Firstly, it is required to write θ_1, θ_2, θ_b, and ψ_2 in terms of the main independent generalized coordinates. Thus, the geometric relations among these dependent generalized coordinates (DGCs) and the independent generalized coordinates (IGCs) can be obtained. The main governing geometric relations can be written along the diagonal line T as Eq. (2).

$$\begin{aligned}(L_1+L_2+d_1)^2+b^2-2(L_1+L_2+d_1).b.\cos(\psi_1)&=T^2\\(L_1+L_2+d_2)^2+\mathrm{Le}^2-2(L_1+L_2+d_2).\mathrm{Le}.\cos(\theta_2)&=T^2\end{aligned}\tag{2}$$

https://doi.org/10.1017/S0263574723000449 Published online by Cambridge University Press

In the above equation, L_1 is the length of the jack's piston and L_2 is the length of the jack's cylinder. Also, b is the length of the triangular chassis and Le is the distance between the two grasped grippers. By solving the above two equations in Eq. (2), θ_2 can be obtained as a function of IGCs :

$$\theta_2 = a\cos\left\{\frac{(L_1+L_2+d_2)^2-(L_1+L_2+d_1)^2+\mathrm{Le}^2-b^2+2(L_1+L_2+d_1).b.\cos(\psi_1)}{2(L_1+L_2+d_2).\mathrm{Le}}\right\}$$
$$\Rightarrow \theta_2 = \Theta_2(d_1, d_2, \psi_1) \tag{3}$$

Now by writing the geometric equation along the X-direction, we have Eq. (4):

$$(L_1+L_2+d_1)\cos\theta_1 + b.\cos\theta_b + (L_1+L_2+d_2)\cos\theta_2 = \mathrm{Le}; \quad \theta_b = \psi_1 - \pi + \theta_1 \tag{4}$$

In the above equation, θ_b is the rotational angle of the robot chassis which can be obtained in terms of the main DOFs (d_1, d_2, and ψ_1). Now by considering the Eq. (5), we have:

$$(L_1+L_2+d_1)\cos\theta_1 + b.\cos(\psi_1-\pi+\theta_1) = \mathrm{Le} - (L_1+L_2+d_2)\cos\theta_2$$
$$\{(L_1+L_2+d_1)+b.\cos(\psi_1-\pi)\}\cos(\theta_1) - b.\sin(\psi_1-\pi)\sin(\theta_1) = \mathrm{Le} - (L_1+L_2+d_2)\cos\theta_2$$
$$A = (L_1+L_2+d_1)+b.\cos(\psi_1-\pi); B = -b.\sin(\psi_1-\pi); C = \mathrm{Le} - (L_1+L_2+d_2)\cos\theta_2$$
$$\Rightarrow A.\cos(\theta_1) + B.\sin(\theta_1) = C \tag{5}$$

Solving the last term of the above equation and substituting Θ_2 from Eq. (3) in the above equation, the following formulation can be obtained which indicates the functionality of θ_1 and θ_b in terms of d_1, d_2, and ψ_1.

$$\theta_1 = a\cos\left(\frac{\pm\sqrt{(A.B)^2+B^4-(B.C)^2}+A.C}{A^2+B^2}\right) \Rightarrow \theta_b$$
$$= \psi_1 - \pi + a\cos\left(\frac{\pm\sqrt{(A.B)^2+B^4-(B.C)^2}+A.C}{A^2+B^2}\right)$$
$$\Rightarrow \theta_1 = \Theta_1(d_1, d_2, \psi_1)\,, \theta_b = \Theta_b(d_1, d_2, \psi_1) \tag{6}$$

Now, ψ_2 can be defined as a function of IGCs in Eq. (7):

$$\psi_2 = 2\pi - \theta_1 - \theta_b - \psi_1 \Rightarrow \psi_2 = \Psi_2(d_1, d_2, \psi_1) \tag{7}$$

Thus, all of the governing relations among the joints of the PSM are determined and all of the passive joints (DGCs) are defined as a function of the main ones (IGCs) which are $\Theta_1(d_1, d_2, \psi_1)$, $\Theta_2(d_1, d_2, \psi_1)$, $\Theta_b(d_1, \mathrm{d}_2, \psi_1)$, and $\Psi_2(d_1, \mathrm{d}_2, \psi_1)$. As a result, the coordinates and movement of all of the robot components can be obtained in terms of the main DOFs. For example, the endpoint of the limb which is the connection point between the gripper and the arm (the wrist coordinate) can be determined by Eq. (8). This point needs to be adjusted using these relations in order to grasp the target pipe.

$$p_{\mathrm{gr}} = \begin{bmatrix} P_{\mathrm{gr}-x} \\ P_{\mathrm{gr}-y} \\ \varphi_{\mathrm{gr}} \end{bmatrix} = \begin{bmatrix} -(L_1+L_2+d_2)\cos\Theta_2 + \mathrm{Le} - \frac{b}{2}.\cos\Theta_b - \frac{b}{2}\sqrt{3}\sin\Theta_b + (L_1+L_2+d_3)\cos\theta_3 \\ (L_1+L_2+d_2)\sin\Theta_2 - \frac{b}{2}.\sin\Theta_b + \frac{b}{2}\sqrt{3}\cos\Theta_b + (L_1+L_2+d_3)\sin\theta_3 \\ \theta_3 + \Theta_b \end{bmatrix}$$
$$\Rightarrow P_{\mathrm{gr}} = P_{\mathrm{GR}}(d_1, d_2, \psi_1, \theta_3, d_3) \tag{8}$$

Therefore, to determine the path motion of the gripper (P_{gr}) in the workspace, the movement of each main joint should be determined. Now to determine the coordinates of the robot's center of mass and the

https://doi.org/10.1017/S0263574723000449 Published online by Cambridge University Press

related orientation in its 2D planar workspace, the Jacobean matrix is employed which can be extracted as follow:

$$J = \begin{bmatrix} \frac{\partial p_{ix}}{\partial d_1} & \frac{\partial p_{ix}}{\partial d_2} & \frac{\partial p_{ix}}{\partial \psi_1} & \frac{\partial p_{ix}}{\partial \theta_3} & \frac{\partial p_{ix}}{\partial d_3} \\ \frac{\partial p_{iy}}{\partial d_1} & \frac{\partial p_{iy}}{\partial d_2} & \frac{\partial p_{iy}}{\partial \psi_1} & \frac{\partial p_{iy}}{\partial \theta_3} & \frac{\partial p_{iy}}{\partial d_3} \\ \frac{\partial \varphi_{iz}}{\partial d_1} & \frac{\partial \varphi_{iz}}{\partial d_2} & \frac{\partial \varphi_{iz}}{\partial \psi_1} & \frac{\partial \varphi_{iz}}{\partial \theta_3} & \frac{\partial \varphi_{iz}}{\partial d_3} \end{bmatrix}_{(3\times5)} \tag{9}$$

In the above equation, p_i indicates the coordinate of the mass center of the robot component i along the X and Y axes on the robot and ϕ_i indicates the orientation of each component around Z-axis which can be defined as a function of IGCs. Note that, two motors are employed to manage the gripper movement. One of them is for setting its angle, and the other one is for locking. During the grasping of the branch, the motor related to set the gripper angle is active. However, once the gripper is locked, this motor becomes passive since its gear is back-drivable. Moreover, the joints which are engaged in the robot path planning are considered as the active joints here, and since this angle is always controlled operatory, it is not employed for path planning of the robot. Considering the mentioned two facts, this motor is not considered as an active joint. So the Jacobean can be employed to calculate the forward kinematics and derive the workspace velocity using the joint space velocity as Eq. (10). Similarly, in order to obtain the required joint space velocity and realize a desired path of the workspace, the reverse kinematics should be solved using the Pseudo-inverse of the above relation.

$$\begin{bmatrix} V_x \\ V_y \\ \omega_z \end{bmatrix}_{(3\times1)} = J_{(3\times5)} \begin{bmatrix} d_1 & d_2 & \psi_1 & \theta_3 & d_3 \end{bmatrix}^T_{(5\times1)} \tag{10}$$

This matrix not only generates the optimal path of the robot but also it can be used to evaluate the actual position of the robot using the sensor feedback installed in the joints of the robot. The actual position shows the operator if the robot is reached the desired operating location. Also, it should be considered that the wrist center is supposed to be controlled automatically here and the rotation of the gripper will be managed manually. That is why the rotation DOF is not considered as the joint space generalized coordinates since its movement needs a high tolerance for covering the grasping process, and this amount of accuracy could not be covered by an autonomous control method. Thus, managing the mentioned joint needs the operator's assistance. Since the system is over-constrained, the inverse kinematics does not have a unique solution and this fact increases the maneuverability of the robot. It means that many configurations are possible for the robot to transfer from one initial point to another one. In order to find an optimum solution, pseudo-inverse is employed here, as Eq. (11). Pseudo-inverse provides the joint space movements, with the minimum required kinetic energy. This method opts here since the required kinetic energy of the actuators is minimum, and thus, the climbing process which needs high potential energy can be realized for a wider range of workspace.

$$\begin{bmatrix} d_1 & d_2 & \psi_1 & \theta_3 & d_3 \end{bmatrix}^T = J^+ [\, v_x \quad v_y \quad \omega_z \,], J^+ = (J^T J)^{-1} J^T$$

$$\Rightarrow [\, d_1 \quad d_2 \quad \psi_1 \quad \theta_3 \quad d_3 \,]^T = (J^T J)^{-1} J^T \begin{bmatrix} v_x \\ v_y \\ \omega_z \end{bmatrix} \tag{11}$$

This is contributed to the fact that, in this way, the power of the actuators can be mostly employed for overcoming the gravitational potential energy rather that producing big kinetic energy with high speed of the joints. The dynamic calculations of the proposed robot are fully extracted and simulated by the same authors in ref. [39]. Here, the full motion analysis of the robot is illustrated and a control strategy is designed and implemented to show the capability of the robot's motion on scaffolds. Also, the dynamics and kinematics of the designed manipulator are extracted by the same authors in ref. [40]. Finally, the

https://doi.org/10.1017/S0263574723000449 Published online by Cambridge University Press

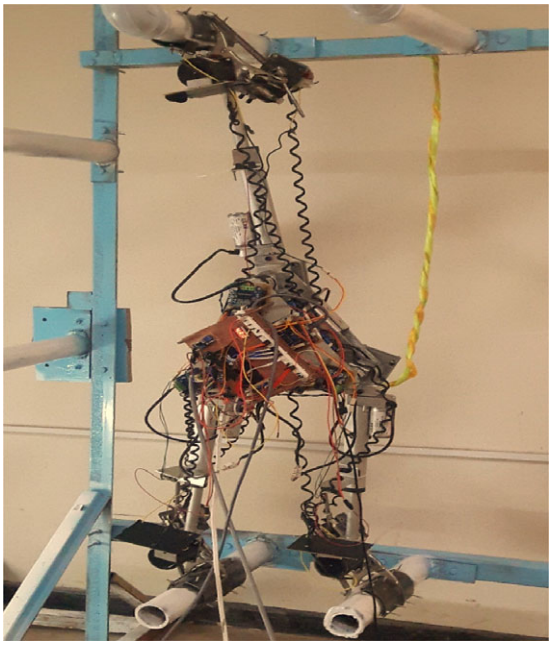

Figure 8. *The manufactured prototype of KharazmBot.*

desired path of the gripper in its planar movement can be determined as a function of the movement of the main DOFs with the aid of these kinematic calculations.

4. Prototype manufacturing

KharazmBot is manufactured at Kharazmi University as a prototype of the mentioned climbing robot. The schematic view of the manufactured robot is shown in Fig. 8.

The process of manufacturing the robot is divided into four main subsections including (1) design and modeling, (2) manufacturing and assembling the mechanical parts, (3) installation of the electrical boards and its related control unit, and (4) design and implementation of a Graphical User Interface (GUI) and its corresponding coding. In the previous section, the first part is covered and the rest process is explained in this section.

4.1. Mechanical parts and assembly

The whole climbing procedure can be realized with the aid of two main motions; first, the chassis motion in which the altitude of the main body increases, and then, the gripper motion in which the gripper moves toward its target and accomplishes the grasping action. For each phase, according to the class of motion, its related fabrication process will be introduced. The CAD model of the designed robot in Solidworks is drawn in Fig. 9 for illustration of the engaged components:

4.1.1. Main body fabrication

Here the components of the robot which are engaged in the main body motion phase are supposed to be manufactured. As explained, the main robot chassis consists of three rotary actuators and three prismatic jacks as the main DOFs. These actuators are configured on three moving limbs of the robot. Also, six rotary actuators are employed as the passive DOFs which are used for grippers. It should be noticed that when the grippers are supposed to get aligned along the pipeline, the wrist motors are on,

https://doi.org/10.1017/S0263574723000449 Published online by Cambridge University Press

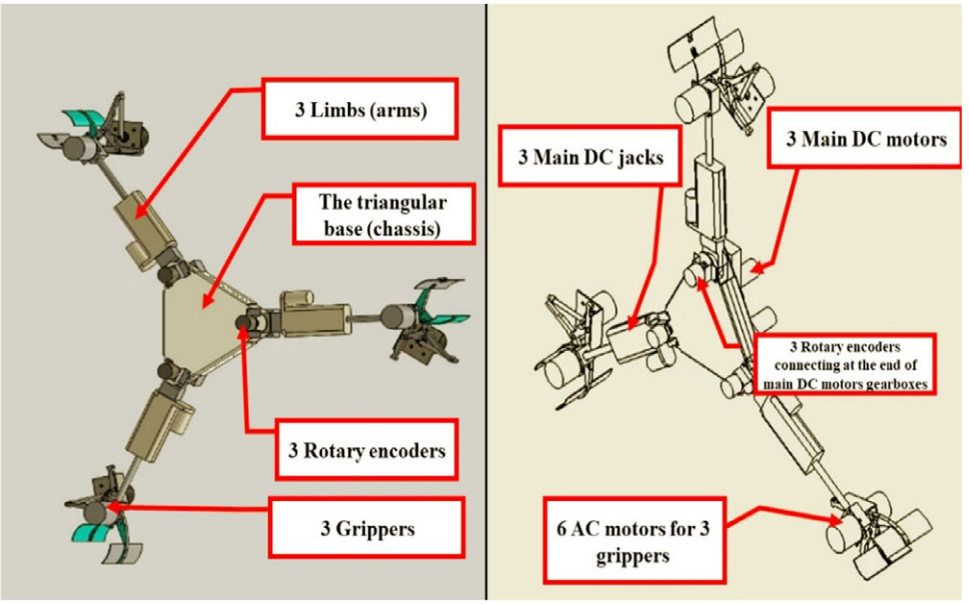

Figure 9. *Schematic view of Solidworks CAD drawing of KharazmBot.*

and when the gripper is locked to the pipe, these motors are supposed to be passive. Thus considering the fact that these motors are back-drivable, they can rotate easily. Also, the motors related to closing and opening the gripper are just active when the gripper is in its transient mode between the open and closed states. By employing the proposed locking mechanism for the gripper, the jaws do not change the state without applying its related command through the designed GUI. For the rotary actuators, the gearbox DC motor of SPGSG46BA 24 V with $i = 470$ is chosen. This motor has an output torque of 17.8 N.m to rotate the arms and orient the main body in the parallel motion of the closed chain robot. The motor shaft is connected to a hard-worked steel (ck45) hollow shaft coupled with two cone-point grub screws. This couple can rotate the aluminum arm interface, that is, the interface between the arm and its attached motor by finger key. Also, the axial slipping is constrained by two ring keys on both sides of the coupling shaft as illustrated in Fig. 10. The robot arm shown in Fig. 11 is a linear jack attached to the brittle aluminum 7000 interfaces by a nut and screw. Figures 10 and 11 show the employed connections between the base chassis and the related jacks. They illustrate the position of the joints and the location of mounting the related actuators on the joints with their corresponding engaged parts. The detail information is illustrated in the figures.

The linear DC motor is a 24 V LINKAN jack with a 1000 N force capacity capable of implementing force along both directions of contraction and expansion.

The power transmission in this motor is a power screw unlike the pneumatic ones and so is not back-drivable. As a result, when the power is off, it keeps its state and is locked. Here these main actuators are connected to three corners of the triangular-shaped robot chassis which is made by two aluminum sheet metals (aluminum 7000 sheets with a thickness of two mm) which are coupled together by bolts and screws. Thus, it forms a tough static structure resistant against bending and torsion due to probable loads. This chassis is the supporting base of the robot through which the three arms are connected by three aluminum hinges as can be seen in Fig. 12. The main rotary motors are installed on the triangular base with the aid of nuts and screws and the motors coupling shafts rotate inside the hinges.

4.1.2. Grippers

The motions related to the gripper have a different actuating process for opening, closing, and rotating the gripper. For each gripper, two AC gearbox motors with a maximum torque of 8 N.m and a maximum

https://doi.org/10.1017/S0263574723000449 Published online by Cambridge University Press

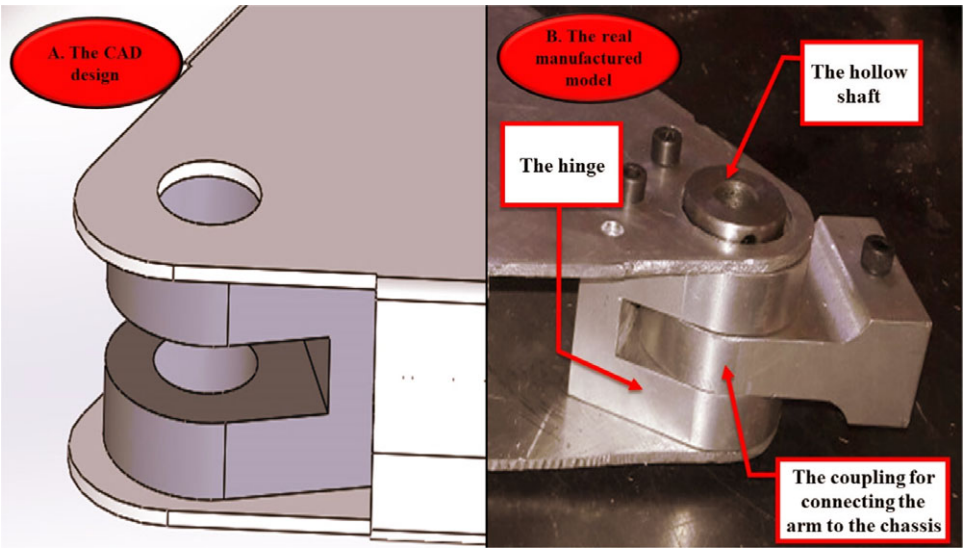

Figure 10. *The connection of the hinge with the hollow shaft and aluminum interface.*

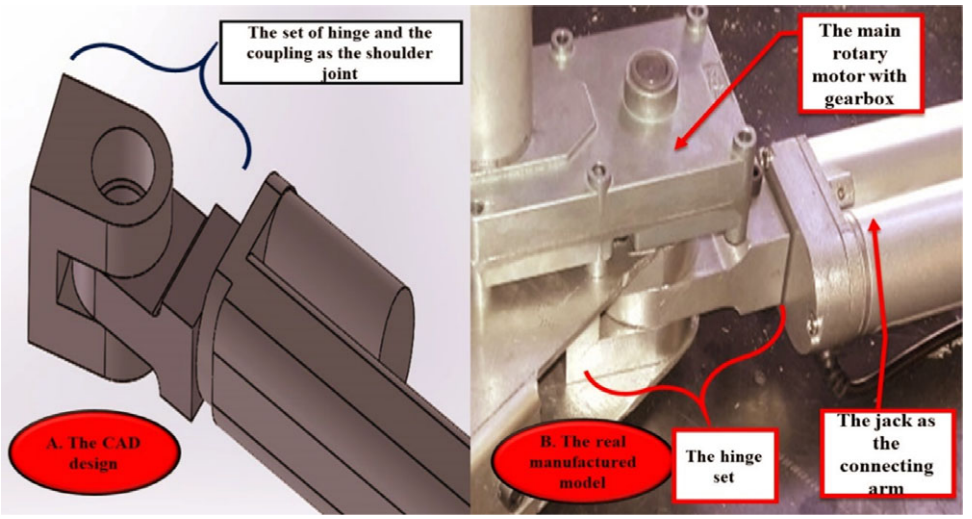

Figure 11. *Connection of the linear jack and the main motor as a shoulder actuator.*

speed of 1.2 rpm are employed. The open/close motor shaft is installed on a slide bar connecting to a phosphor-bronze cylindrical slider which can move along the slide bar frictionlessly in order to open or close the gripper's jaws according to the motor direction. The mechanism of the gripper is designed in a way that, if the related actuating motor rotates clockwise, its corresponding locking plier will be fastened and vice versa. Thus, the operator is able to decide to fasten or open the locking plier by choosing the direction of the motor rotation which is available through the provided GUI.

The gripper's jaws or fingers have been widened with arc-shaped components of steel pipe in order to grasp the target point firmly without the possibility of falling or slipping. The jaws are equipped with rubbers for increasing the static friction coefficient, and the metal part is teeth shaped in order to bite the rod and decrease the possibility of slippage. The frictional coefficient increases by using the mentioned rubber since the damping coefficient of the contact surface increases. The whole gripper rotates by another AC motor (wrist actuator) to orient the gripper in its planar workspace and to guide

https://doi.org/10.1017/S0263574723000449 Published online by Cambridge University Press

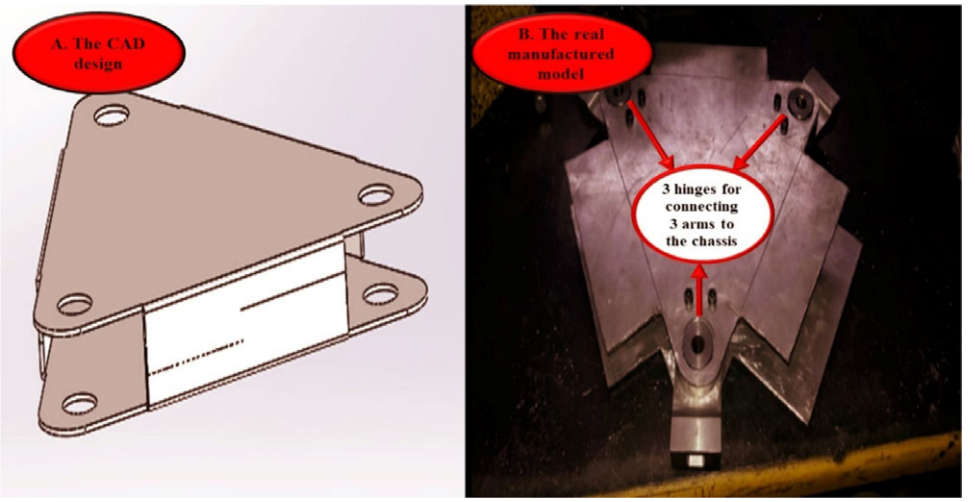

Figure 12. *The chassis of the robot with its three hinges for connecting to the related limbs.*

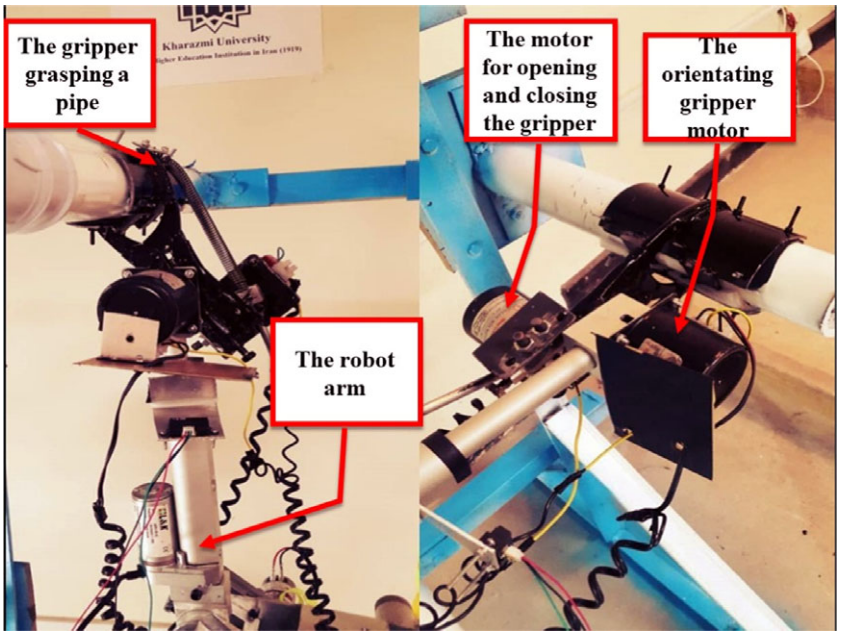

Figure 13. *The prototype of the manufactured gripper for KharazmBot.*

the gripper to the aim point of grasping. The connection between the grippers and the AC rotational motors is realized by a hollow shaft. The grippers and their related AC motors are attached together with the aid of some cone-point grub screws. The prototype of the manufactured gripper installed on the robot's limb is shown in Fig. 13.

Considering the fact that rubber is a kind of elastomer, it has a high viscoelasticity property and consequently shows a high resistance against increasing the velocity or slippage with respect to a base material. Thus, for the proposed gripper, whenever the gripper is supposed to be rotated as a result of an external torque, the related implemented energy will be damped as a result of adhesion and hysteresis property of the rubber. Moreover, the frictional coefficient of the rubber and also its normal contact force between the gripper and steel is high as a result of using the proposed locking plier mechanism, and thus,

https://doi.org/10.1017/S0263574723000449 Published online by Cambridge University Press

Table I. *Characteristics of actuators.*

Actuator type	Voltage	Weight (kg)	Max speed	Maximum torque, force	Duty	Number
SPGSG46BA Gearbox DC motor	24 V, DC	1.36	16 RPM	17.6 N.m	Main rotary actuator	3
Linkan LA25.1-15-24 DC motor	24 V, DC	0.9	2 cm/s	1000 N	Main linear actuator (arm)	3
Single-phase AC motor	Single phase, 220 V, AC	0.5	1.2 RPM	8 N.m	Open/close and gripper rotating motor	6

the produced frictional force prevents the gripper from slippage. More details about the force analysis of this novel gripper are conducted in ref. [38], and it is shown here by modeling the statics and kinematics of the gripper that the proposed gripper can overcome the weight of the robot. The characteristics of the robot's actuators are demonstrated in Table I.

4.2. Electronics and control unit

4.2.1. Electronics

The robot's actuators are divided into two groups DC and AC. For DC circuits, a 24-V and 20 Amp switching electronic power (an AC to DC converter) is considered to generate the required DC electronic power. Thus, all of the 24 V DC actuators are fed using the same voltage with the aid of a parallel connection of circuits. Since the motors are supposed to be controlled, the connection between the motors and the electronic power source is not direct. Some driver modules are used to provide the electronic currents from the power supply for the DC motors according to the required voltage and current needed for their related special motion of the motors. For this robot, six IBT-2 H-Bridge DC driver modules with MOSFET chipset are considered which can tolerate 43 Amps and control the 24 V DC motors in the forward and backward directions. The amount of the output voltage is defined by the input signal from the controller. For the AC motors of the gripper, AC power is considered as the power source without any interface. A dimmer is employed to prevent the sudden voltage and current drop for the DC motors which are connected to the same AC plug (the switching and AC wires for the gripper's motors have the same AC power source).

4.2.2. Control unit of the main body motion

The main controller which provides the controlling signals for all of the actuators and receives the signals from the sensors is Arduino Due microcontroller based on Atmel ARM architecture microchip with a frequency of 83 MHz and memory of 512 KB which is enough to write the required program in Arduino IDE based on Java and C programming language. Since the ARM architectures are known as a fast and precise microcontroller, they can be employed in such complex robots and systems and can handle heavy kinematic calculations in an online way toward controlling the robot. Also considering the fact that a gearbox with a high ratio of 400 is employed for the motors, the rotational speed of the joints can be decreased to the maximum value of 16 rpm with a smooth function. Thus since the encoders are installed on the output shaft of the gearbox, the data transfer of this rotational speed is completely possible with acceptable accuracy. The mentioned microcontroller has enough pins of PWM signals for position control of the actuators. The control center of the first version of the designed robot is semi-autonomous. Since the robot needs to grasp the branches by its gripper and this process requires high accuracy, the probable errors need to be compensated. The proposed controlling strategy is to move

https://doi.org/10.1017/S0263574723000449 Published online by Cambridge University Press

the robot to the desired destination using the kinematics of the robot and compensate its corresponding errors using feedback control. The employed closed-loop controller for controlling the manufactured climbing robot of KharazmBot is a PD controller by which the required PWM signals of the motors can be calculated using position error and its related derivation. Thus, the required PWM can be calculated as follow:

$$\text{Input} = \text{PWM} = K_p(e)e + K_d(e)e \tag{12}$$

Here $K(e)$ is the controlling gain by which the joint space displacement can be converted to the required PWM of the motor and is a function of the instantaneous error of the joints. Since the integrator term increases the oscillatory response of the arm and thus is not suitable for the cases in which the end-effector should be controlled in an over-damped condition, this term is not employed here. The desired position of the robot during the locomotion and manipulation is also calculated by the control center. Here the index p denotes the proportional gain and the index d is related to the derivative one. e is the error of the joint rotation. Moreover, the PD controlling gains are a relay function of the related errors:

$$\begin{aligned} &\text{if } |e| < 8 \; K_p = 7, K_d = 3.\ldots \\ &\text{else if } |e| > 8 \Rightarrow K_p = 10, K_d = 5 \end{aligned} \tag{13}$$

The above stepwise tuning of the controlling gain increases the smoothness of the robot's performance and decreases its chattering phenomenon. The constant values of controlling gain are tuned according to Ziegler Nichols method to guarantee the stability and accuracy of the controller and decrease the overshoot and settling time of the system. Here for the position control of the main rotary motors, three encoders are employed to sense the exact position of the output shaft of the motors which are installed at the output hollow shaft after the gearbox. The encoders are of (A/B) type which can sense both directions of motion with a resolution of 600 pulses per revolution. Thus, a total 1200 pulses can be achieved per 360° of rotation. This is contributed to the fact that the employed encoder is of type A/B which indicates the direction of the rotation and thus the pulses are multiplied by two. Since the Arduino Due microcontroller is equipped with digital pins which can be considered interrupt pins, each pair of encoder signal wires can be connected to these digital pins as the interrupt pins. Therefore by receiving the signals from the encoders and command line, it is possible to compare the data and calculate the related errors. Afterward, the PWM signal can be generated with the aid of the microcontroller according to Eq. (12). The signals will be then sent to the motor drives to realize the proper tracking of the rotary motors. The control strategy for linear motors is also the same except that this time the positions of the jacks are measured by sharp sensors (IR distance sensor) that can measure the distances between 4 cm and 30 cm. The sharp sensor is installed on the jack, and a plate is attached to the gripper which can receive the IR light from the sharp sensor and estimate the distance. The sensors are connected to the analog pins of the Arduino by which the voltage signal from 0 to 3.3 V of the sharp sensor can be converted to distance estimations. Now by calculating the error and employing the above-mentioned PD controller, the closed-loop motion control of the jacks is fulfilled.

4.2.3. Control unit of grippers

As was explained before, each gripper consists of two AC motors. The first one supplies the power of its rotary motion while the other one is responsible for opening and closing the jaws. Since the motors are AC with low speed, here the position control is not mandatory. Only the required time and direction of these motor movements should be easily controlled by the operator through the related GUI in order to grasp the pipe. Actually, the AC motors are controlled manually by the operator based on the motion feedback sensed by the user's vision.

Therefore, for each AC motor, a two-channel AC relay module is employed to stop and run the motors and change their related directions. The relay module is connected to the digital pins of the Arduino and the corresponding logical signals enable or disable the relay channels. In fact, the relay is the interface

https://doi.org/10.1017/S0263574723000449 Published online by Cambridge University Press

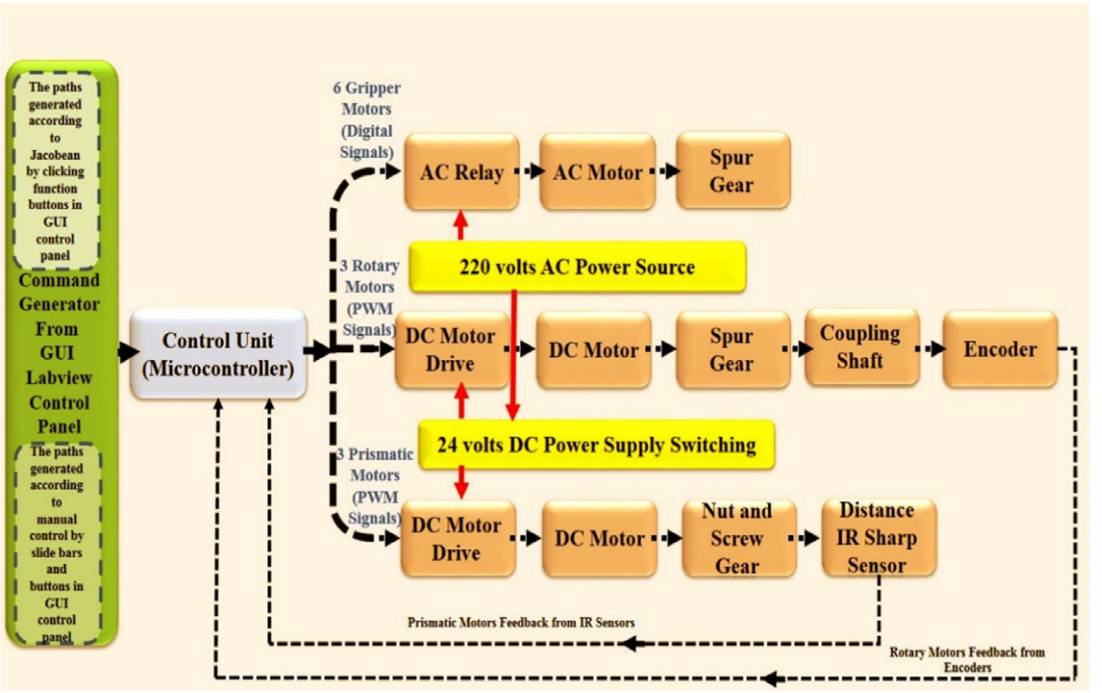

Figure 14. *The control block diagram of all of the actuators in KharazmBot.*

between the AC power and the AC motors and indicates the channel by which the AC current should be run. The user can choose the proper channel in order to change the direction of the related AC motor rotation either for the open/close procedure or to determine the gripper wrist direction for implementing the alignment. The whole robot's control strategy for all of the actuators is illustrated as a total control diagram in Fig. 14.

4.3. Command generator and power supply

4.3.1. Command generator

For the command unit, a GUI is designed as the required control panel by which the operator can handle the robot's motion. The handling can be totally autonomous or semi-autonomous. The designed GUI panel for the robot consists of some graphical slide bars and buttons through which the desired path can be fed to the robot by defining the main motor trajectories and also defining the state of the grippers. For the motion control of the main actuators, two strategies are defined in the designed GUI. The first one is the manual approach in which the operator moves the slide bar proportional to the required movement of the actuator by the designed slide bars in the GUI. In the second approach which is automatic, the desired function of the actuator movement can be imported as a function of time.

The best GUI interface for this robot is LabView which is fast and has a real-time graphical programming environment. The command signals are generated in the form of a sequent of strings in the LabView software. They will be then transmitted through the serial ports from the PC to the Arduino serial pins by RS-232 serial interface with a TTL converter which converts RS-232 signals to RX, TX type and is readable or writeable for Arduino serial pins. All of the states and demands for all of the motors are set in a serial signal in a string format which can be sent to the microcontroller at a baud rate of 115,200 bits per second. This speed is fast and wide enough for real-time communication through the serial data transfer protocol between the PC and microcontroller. In Fig. 15, the main designed controlling panels that are programmed by the LabView are shown through which the motors and jacks can be controlled according to the desired destination of the robot.

https://doi.org/10.1017/S0263574723000449 Published online by Cambridge University Press

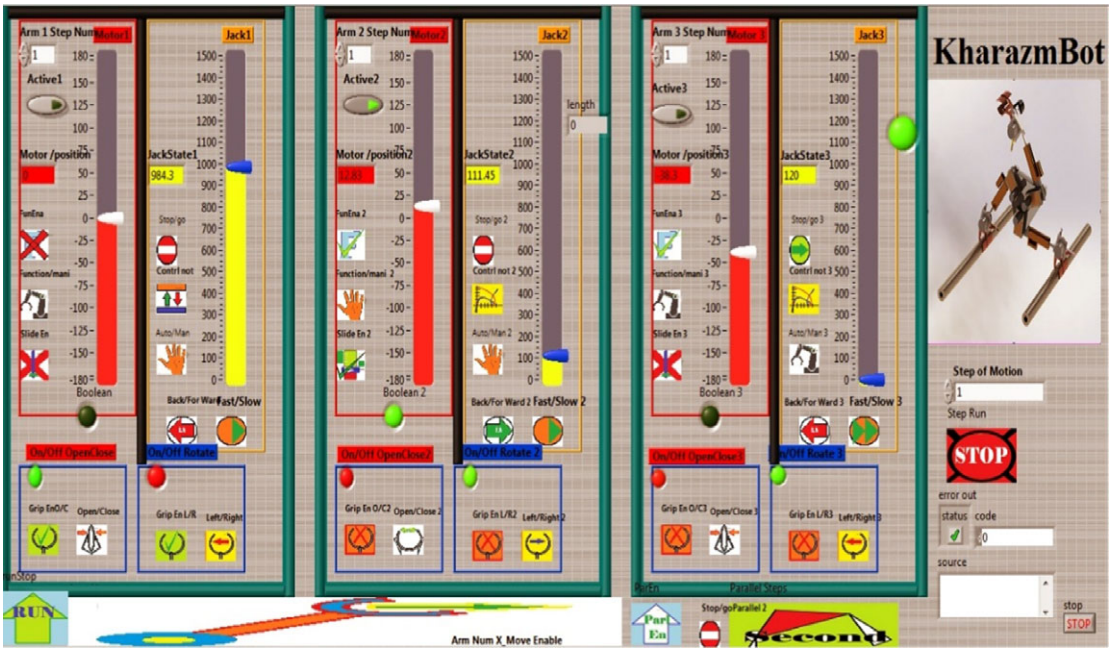

Figure 15. *The control panel GUI in LabView.*

Therefore, here for the robot in its current form, the operator should control the system using the mentioned GUI for the structures for which, whole the workspace is observable, and thus, the operator according to the instantaneous location of the robot together with the observed structure can distinguish that what is the next target pipe for the robot gripper. Here just a webcam needs to be installed on the gripper through which the operator can adjust the gripper position during the grasping process with respect to the pipe by checking the situation in the related monitor.

4.3.2. Microelectronic power supply

All microelectronic parts such as the motor driver, enable chipsets, distance sensors, encoders, relays, and TTL converter should be fed with a 5-V DC power source which can be done either using batteries or employing voltage regulators.

As there are numerous microelectronic parts in the robot including six relays, three distance sensors, three encoders, six motor drivers chipset enable, and one TTL converter, a voltage regulator (DC to DC voltage reducer) is employed in this robot which converts the 24 V switching power source to 5 V for the mentioned microelectronic parts with one Amp current limitation. The Arduino itself is fed by a 5-V USB serial cable connected to a PC. The whole robot parts with their corresponding sets of connections between the mechanical parts and its electronic parts are shown in the graphical diagram of Fig. 16.

5. Experimental verification

In this section, in order to check the efficiency of the proposed and manufactured robot toward climbing the infrastructures, a test bed is designed and manufactured similar to the pipeline infrastructures from which the climbing robot is supposed to move through. This test bed is made up of several steel pipes with diameters of 6 cm installed at different heights through which an increase in height level can be realized by the aid of the fabricated robot. Here the vertical distance between the pipes of the test bed is about 560 mm, and the total height of the test bed is about 1500 mm. The structure of a real scaffold can be realized by repeating the pattern of this test bed. Here according to the employed path,

https://doi.org/10.1017/S0263574723000449 Published online by Cambridge University Press

Table II. *The physical characteristics of the KharazmBot and test bed.*

Parameter	Description	Value	Unit
M_b	Base mass	5	kg
M_g	Gripper mass	1.8	kg
M_a	Arm mass	1.1	kg
M_t	Total mass of the robot	13.7	kg
S_j	Jack stroke	150	mm
A_m	Main motor angle limitation	180	Degree
B	Length of the triangular basis side	300	mm
d_{jc}	Contracted jack length	330	mm
d_{je}	Expanded jack length	480	mm
d_g	Gripper length	130	mm
d_s	Stand's step length	560	mm
d_p	Pipe diameter	60	mm
G	Gravity acceleration	980	mm/s^2

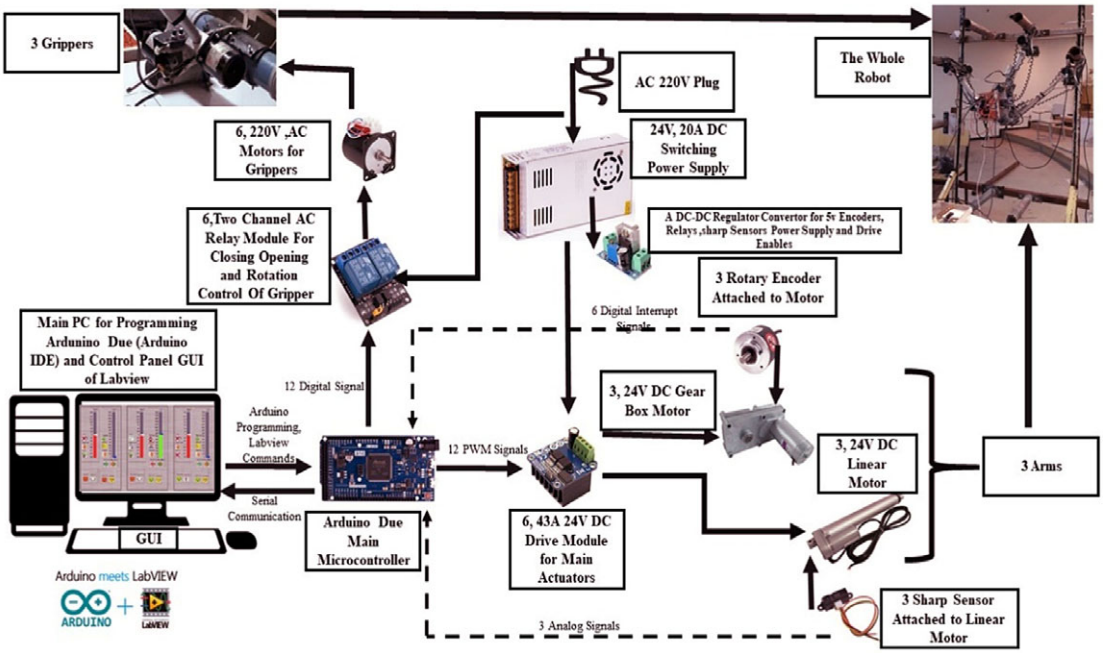

Figure 16. *Hardware and software architecture of the designed system.*

the beneath grippers have traveled about 1200 mm to reach the upper pipes. This is a single step of motion that is performed for 250 s. The speed characteristics of the robot are shown in Table I. Thus, it can be concluded that the robot has a traveling speed of about 5 mm/s. Here as mentioned, the stability of the robot has more priority than its speed. It means that to have higher speed, some more powerful actuators should be employed to implement big torques or forces without losing their speed. For declaring the geometry of the test bed, the dimensional details are shown in Fig 17. Also, Tables I and II show the conditional characteristics such as the actuators' speed and the gate distance through which the robot moves.

The structural configuration of the test bed is shown in Fig. 17. This structure is a sample of a planar test bed, and the operational performance of this robot is not limited to this pattern. The robot can climb

https://doi.org/10.1017/S0263574723000449 Published online by Cambridge University Press

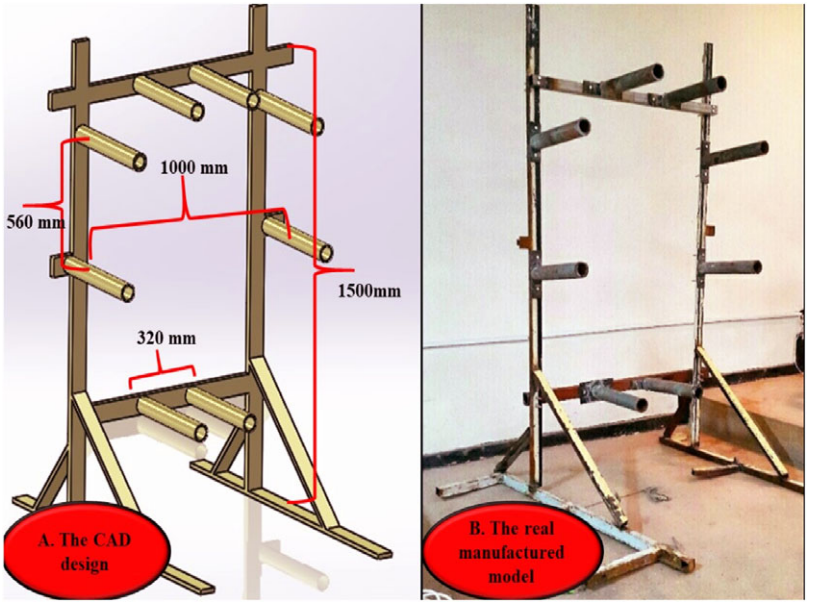

Figure 17. *The constructed test bed for the experimental tests.*

through any 2D pipeline infrastructure. The plane of this structure can have any direction with respect to the earth. The plane just should be perpendicular to the pipeline's direction.

A path is planned for the robot by which the height of the robot can be increased. The ascend will be realized with the aid of the explained maneuver of the system within the pipelines using the limbs and grippers. The climbing strategy is based on a step-by-step motion, and by the complete accomplishment of these steps, the overall climbing procedure will be fulfilled.

Therefore, for each step of motion, a simple path planning should be performed as the desired trajectory of the robot. First, the structure of the pipeline frame and its geometric specifications should be defined. The coordinate of each pipe is supposed to be predefined by the designer. Hence, by knowing the coordinates of the pipes, path planning can be conducted using the kinematics of the system. Thus, the desired trajectory of each actuator can be obtained using the inverse kinematics for each motion step. Finally, the paths are imported through the designed GUI in a semi-autonomous way. The generated path through the kinematics is set as the desired trajectory. This trajectory is then tracked in an autonomous way, and its final error will be then improved manually by the operator. The climbing strategy can be summarized as the flowchart shown in Fig. 18.

5.1. Climbing movement

As was explained, since the robot is redundant, the path between the two boundaries is not unique. Here, the dynamics of the robot are considered in order to choose an algorithm for the climbing procedure. The path should be considered so that the required amount of the actuator powers does not violate their related allowable bounds. So, a pre-simulation with actual robot characteristics is required to check the mentioned constraints. In order to perform the experimental tests, according to Fig. 14 and the flowchart of Fig. 18 the optimal solution of the joints is extracted using the pseudo-inverse of the robot Jacobian and its related path is fed to the robot as the desired trajectory. However, a switch is designed to alter the controlling strategy from the autonomous state to the operatory one in order to manage the robot during its movement through uncertain environmental situations. In these situations, the controlling of the robot's movement through its desired path needs to be checked by the operator, and it should be improved by interfering with the operator's auxiliary commands using the GUI. Both the autonomous

https://doi.org/10.1017/S0263574723000449 Published online by Cambridge University Press

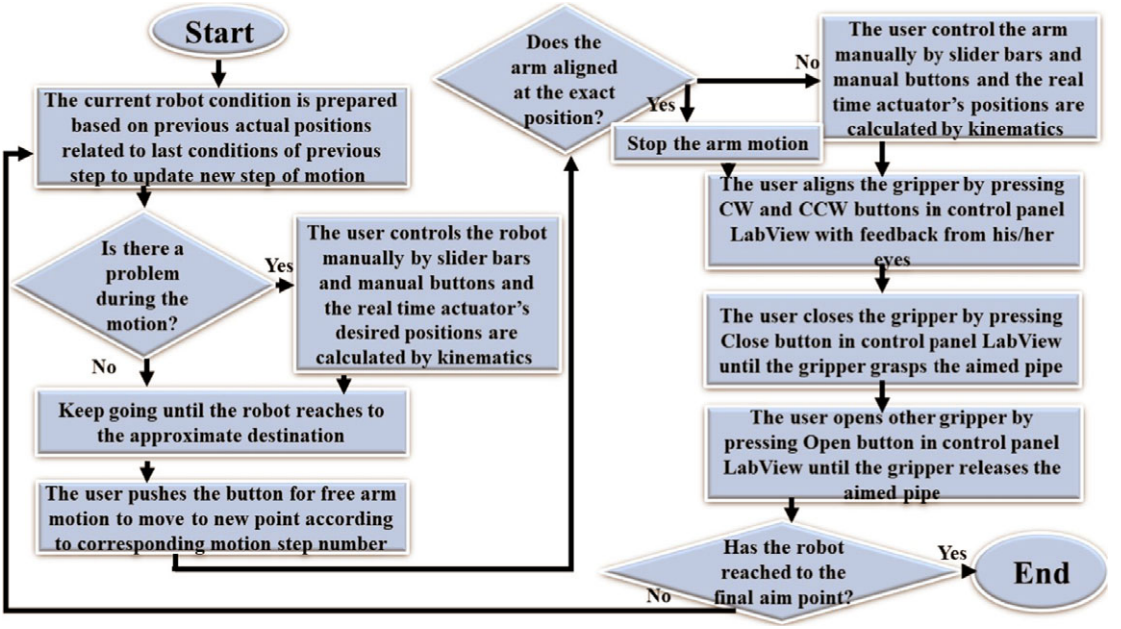

Figure 18. *Block diagram of the climbing strategy.*

and operatory controlling algorithms employ PD controllers to compensate the errors. It should be also noticed that considering the fact that the robot is over-constrained, the actuators need to be perfectly synchronized in order to prevent the robot from being locked. Covering this ideal condition is practically impossible, and thus, here the active and passive actuators are sequentially switched in a way that the number of active joints would be equal to the number of DOFs of the robot. In each duration, the active joints are controlled to move through their related desired path while the passive ones are off and act as a free joint. These passive joints will move obligatory through their desired path in this way. The role of the active and passive joints is defined by the operator either during its autonomous mode or during its manual mode according to Fig. 18. In the latter case, this switching is done according to the environmental situation while the number of them is always unchanged and is equal to the DOFs of the robot. The physical characteristics of the robot and its related test bed are shown in Table II. The mentioned path is tracked by the simulated robot in MSC-ADAMS in order to check the ability of the robot toward covering the required maneuver of this path through the manufactured test bed. The required range of motors' torques is evaluated using MSC-ADAMS as Fig. 19 during its five motion steps which are within the allowable bound of the provided actuators. In Fig. 19, the required torques of the motors and the forces of the jacks are shown for a specific path that moves the robot from the downstage to the upstage of the test bed.

In above Table, d_s is the vertical projection of the distance between the pipes. As can be seen from Fig. 19, one can conclude that all of the actuators' torques are within their allowable bound according to Table I. It can be seen that the maximum torque is related to step three for motor F which is 13 N.m and the maximum force is related to step two for jack C which is about 165 N.

The climbing process of the robot in MSC-ADAMS can be seen in Fig. 20 which is shown in five steps. As can be seen, the overall movement of the robot can be covered according to the pre-simulation. This simulation shows that the planned path can be really tracked by the fabricated climbing robot in order to move through the manufactured pipeline structure.

In order to conduct the experimental test, the robot is located at its initial position in which two limbs are locked to the lower pipelines. Then, the designed GUI is run and the desired paths are commanded to the controller according to the flow chart of Fig. 18 through the serial communication ports.

https://doi.org/10.1017/S0263574723000449 Published online by Cambridge University Press

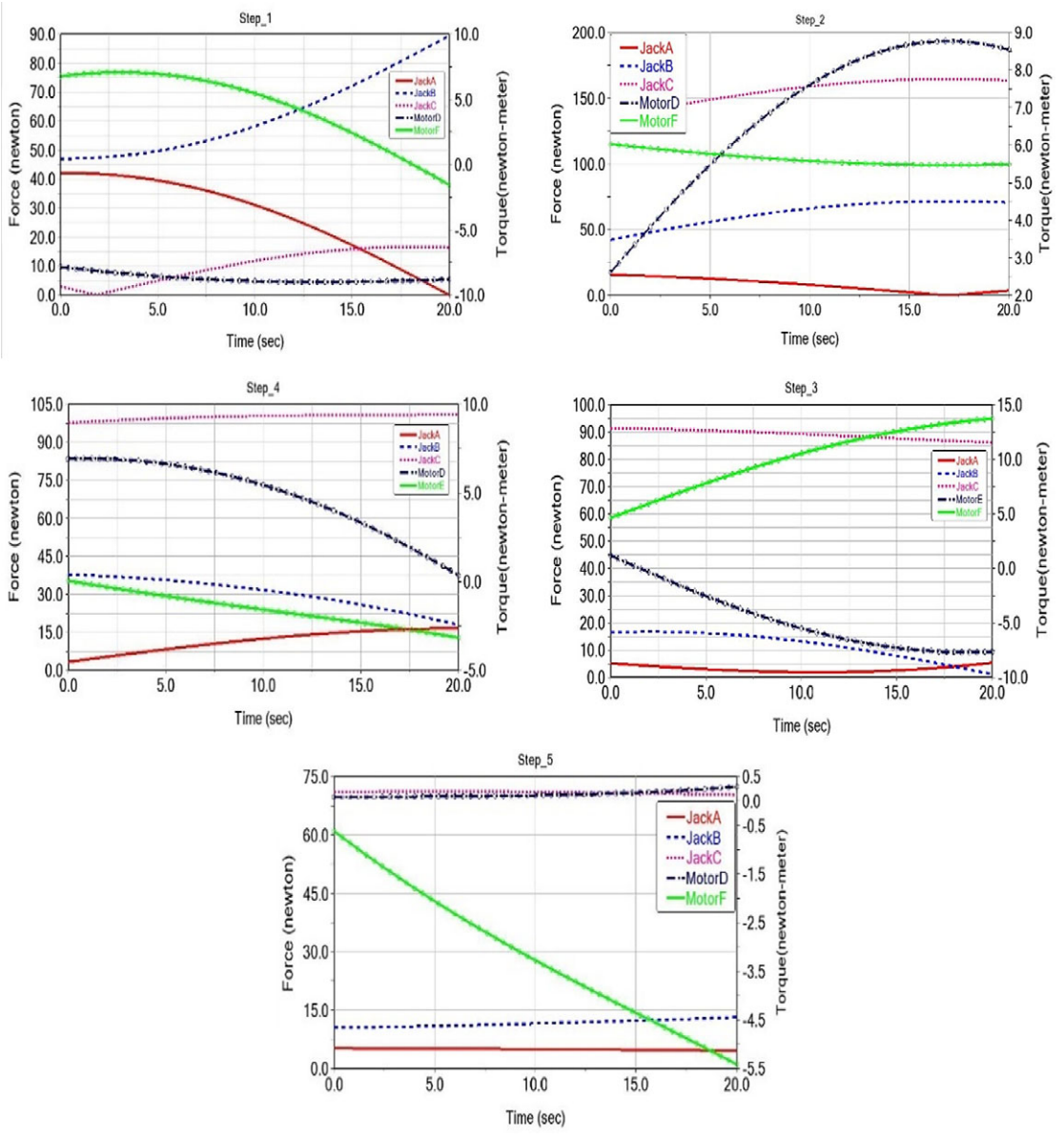

Figure 19. *The required torques and forces of the main actuators for five steps of motion during the climbing procedure through the predefined path in MSC-ADAMS simulation.*

The controlling signals of the main actuators are PWM calculated in the microcontroller based on PD control algorithms described in Section 4. For the secondary actuators, however, which are the grippers' AC motors, the digital signals are generated according to the received commands from the GUI. The related controlling block diagram can be seen in Fig. 14. The actual data of the main actuator motions are also recorded and sent to the controller simultaneously with the aid of the installed sensors which are explained in the previous section. The actual movement of the robot is captured based on the defined motion gaits and is shown in Fig. 21. As can be seen, these series of motion gaits are considerably compatible with the desired configurations of the robot which was simulated in MSC-ADAMS. The robot moves from the initial position at gait 1 to the final position and configuration at gait 12.

https://doi.org/10.1017/S0263574723000449 Published online by Cambridge University Press

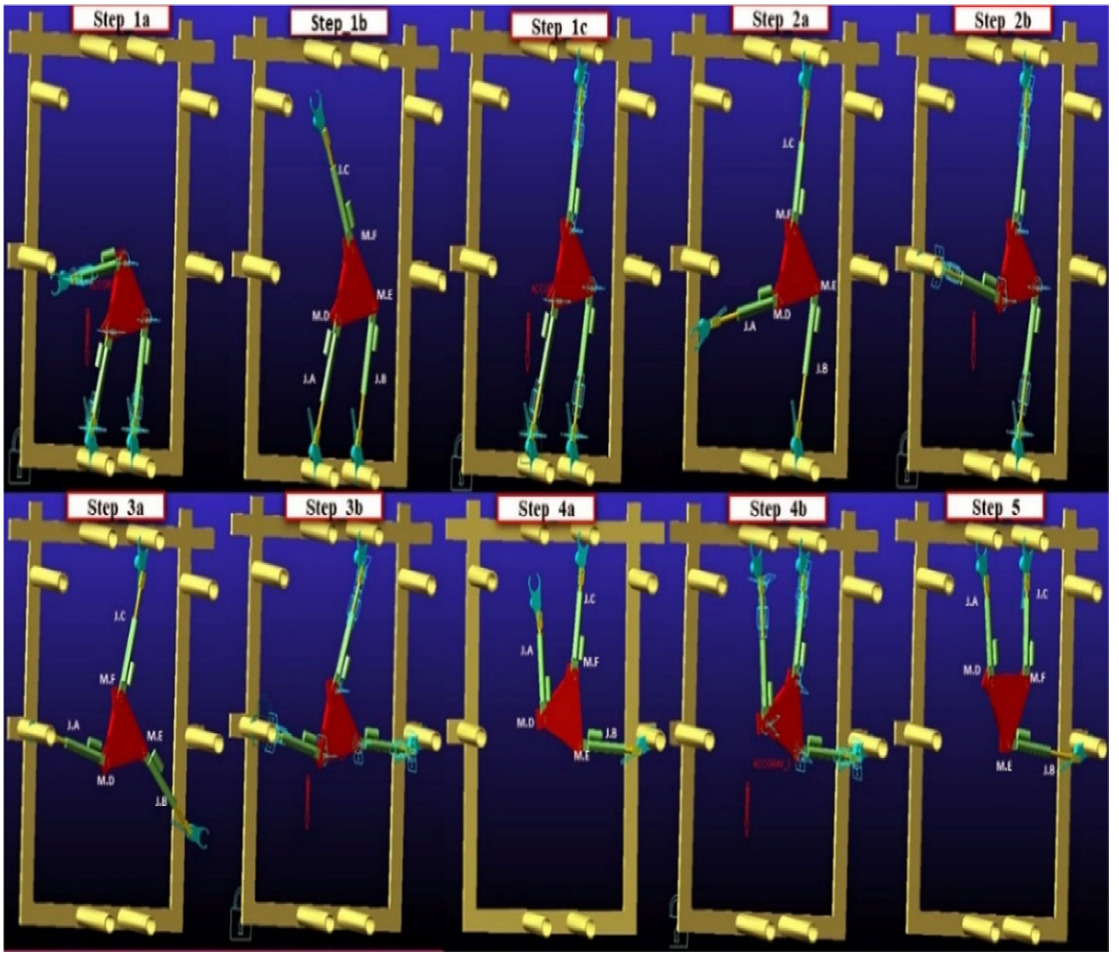

Figure 20. *Simulation of KharazmBot motion in MSC-ADAMS.*

This experiment proves that the robot is able to ascend through the structure with good maneuver and high stability as it was claimed in the robot design section.

Since the actuators' power is constant, the movement speed of the robot during those stages of the movement in which higher force or torque is required is slower. Thus, the actuators should be opted for the worst case in which the highest amount of force or torque is required which is extracted in the simulation study as can be seen in Fig. 19. Here according to the selected motors of Table I, the movement and speed of the robot is studied. In order to check the accuracy of the robot traveling to its desired destination, it is required to compare the desired commands of the actuators with the actual movement of the robot recorded through the sensors.

The angles and lengths of the robot's actuators are shown in Fig. 22 in a sample configuration of the robot. A comparison of the actuator movements between the desired motion of the rotary motors and the actual data captured by the encoders is depicted in Fig. 23 (right side). The same comparison between the desired linear movement of the jacks and the corresponding data of the IR distance sensors can also be observed in this figure (left side). Here the responses of all of the motion gaits of the robot are depicted serially. As can be seen, in each step, five actuators are active while the sixth one is passive. It should be noticed that the desired path of all of the joints consisting of the passive one is extracted using the command signals of the operator based on the kinematics of the robot.

Also, it can be observed that the desired set-point of some joints is stationary, and thus, a regulatory movement needs to be accomplished, while the set-points of the other ones are time-dependent, and

https://doi.org/10.1017/S0263574723000449 Published online by Cambridge University Press

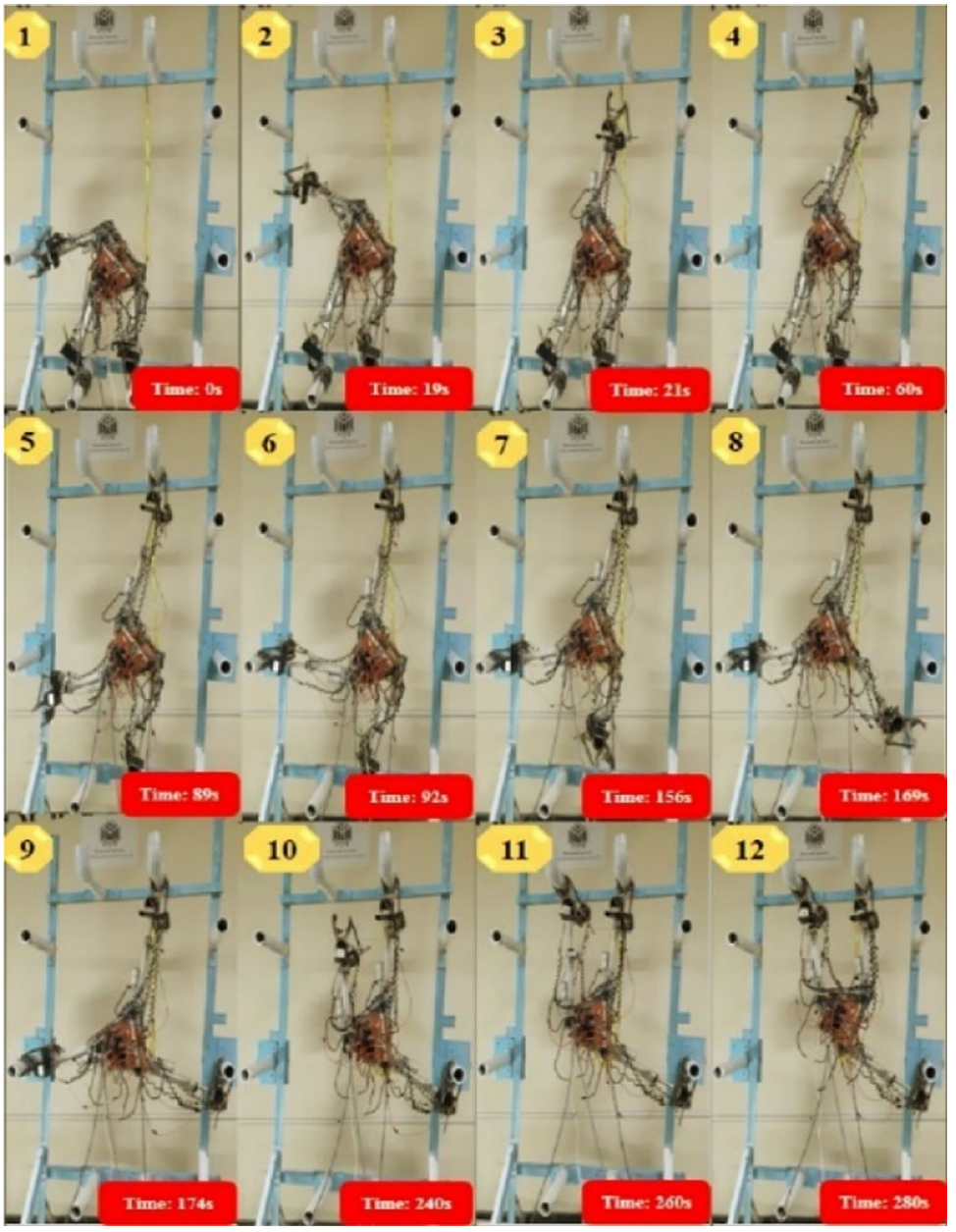

Figure 21. *Actual movement of KharazmBot in an experimental test with twelve motion gates.*

thus, a tracking control should be implemented on them. It can be seen that the tracking accuracy of the joints' rotation is satisfactorily fulfilled, and the maximum error does not exceed 10° for rotary motors (motor D). This shows that the robot's location is compatible with the desired one. The ignorable vibrational response of the actual data is contributed to the accuracy of the employed encoders and the environmental disturbances. For the jack response again, here the maximum error is about 7 mm which is ignorable and satisfies the required tracking of the linear joints precisely. It can also be seen that the movement of the linear jacks is realized with smooth slopes while the slope of the rotary motors' movements is sharper for the whole duration of motion in the climbing procedure shown in Fig. 23.

https://doi.org/10.1017/S0263574723000449 Published online by Cambridge University Press

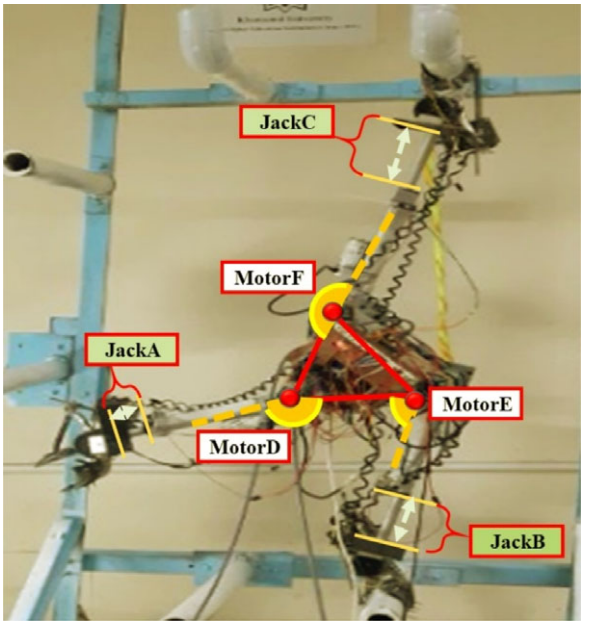

Figure 22. *Considered angles and lengths of the robot with its related main actuators.*

This is contributed to the fact that the speed of the jacks is considerably lower than the rotary motors as a result of their employed power screws. Generally, it can be concluded that the movement of all of the actuators is roughly smooth since all of them are equipped with a gearbox that damps the main amplitude of the vibrations. For more investigation of the tracking accuracy during the robot climbing, the error of tracking and regulation control is shown in Fig. 24.

These values are the average filtered errors of the system. It can be seen that the error amplitude of both the rotary and linear actuators are within the allowable range which shows the efficiency of the designed and implemented controller. The maximum error of the rotary actuators is averagely about 5°, and the maximum error of the linear jacks is averagely about 5 mm.

According to the good accuracy observed in the results, one can conclude that the actuators are opted for the worst case in which the highest amount of force or torque is required. This fact is extracted through the simulation study as can be seen in Fig. 19. Here since the stability is in the priority, the speed of the system is low as a result of constant power of the actuators, and thus according to the selected motors of Table I, the movement profile of the robot is according to Fig. 23 which has an acceptable accuracy.

On the other hand, it can be seen that the error profiles of the linear sensors have more vibrational behavior compared to the rotary ones. This is contributed to the fact that the IR sharp sensors employed for the jacks are more impressible from the noise sources while the encoders are more accurate due to their isolated structure and the strategy of action. But since the more accurate measuring requires more time, the control speed reduces which can result in considerable delays and affect the robot's motion. Thus, the main noises of the sensors need to be filtered through the microcontroller using the average filtering method. The average filtering method is a conventional method for filtering the noises' amplitude. This approach is opted here since the employed sensors for manufacturing the prototype of the robot are not very accurate, and it is required to neutralize the effect of random deviations of the signals with respect to the actual data. Hence, the oscillations of the IR data are mostly related to the noises while the observable oscillations related to the encoder profiles are contributed to using PD controller for controlling the joints which produces an overshoot on the performance of the joints. Sudden jumps of the error profiles are also related to the accidental movement of the robot parts which are affected by the gravity force. These errors are however quickly compensated with the aid of the implemented PD controller. In order to neutralize the destructive effect of the sensor noise on controlling the system, the

https://doi.org/10.1017/S0263574723000449 Published online by Cambridge University Press

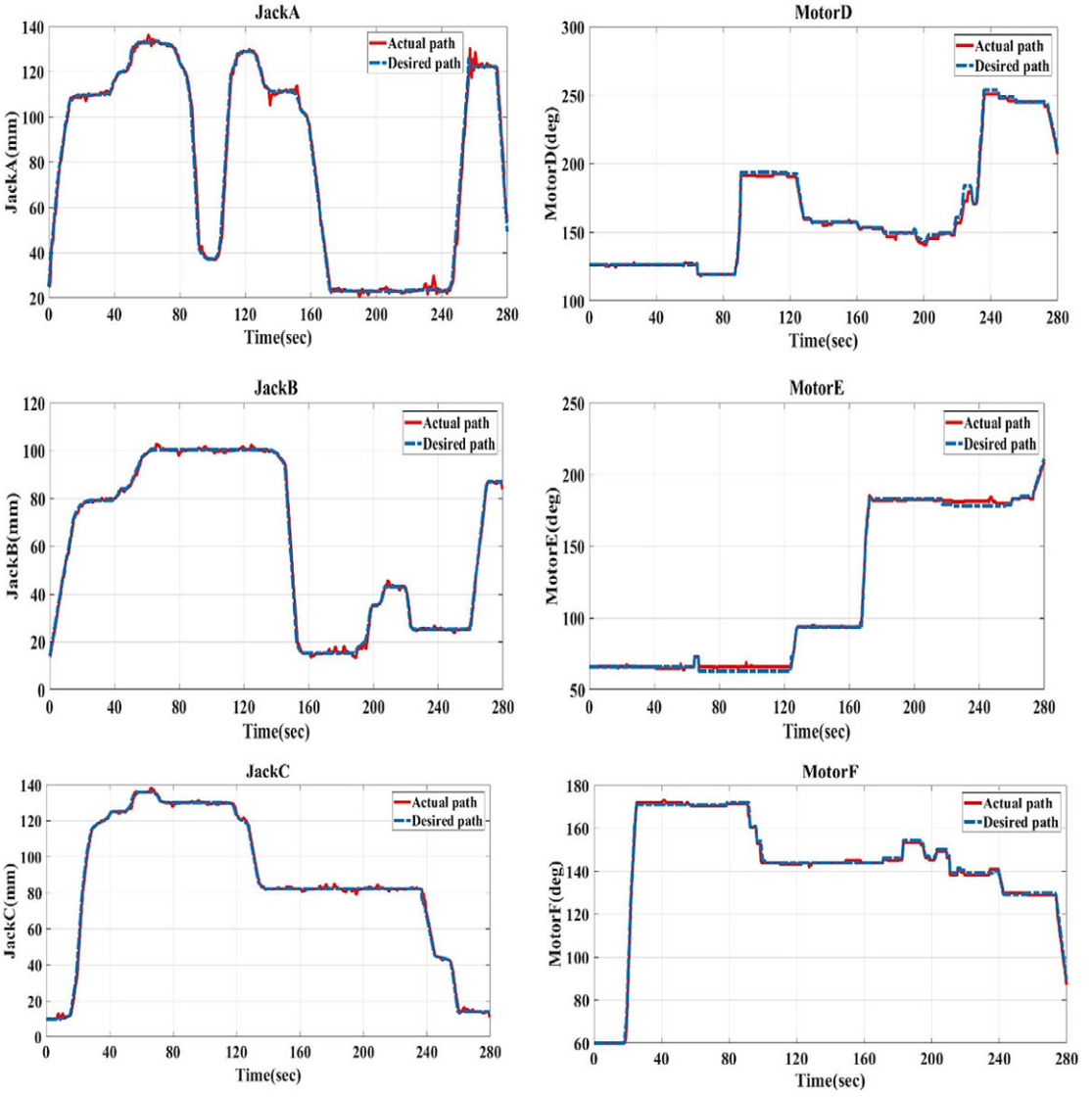

Figure 23. *The comparison between the actual and desired path for all of the actuators.*

controlling gains of the designed PD controller are defined as a function of error in which for small errors related to the noise, the gain is set to zero, and thus, the chattering phenomenon is canceled. However, it can be seen that the main errors related to the dynamics of the system are fastly compensated using the implemented PD controller.

5.2. Manipulating movement

Also in order to show the ability of the designed robot toward accomplishing the inspectional or operational tasks, at the last step after finishing the climbing process of the robot, the free limb of the robot is moved freely within the workspace with the aid of the chassis motion, to guide the manipulating tool toward the target. This process can be seen in the following scenario as in Fig. 25.

Hence, the following overall change of configuration in the robot workspace is realized as the result of combining the robot climbing movement phase and the robot manipulating movement phase, as shown in Fig. 26.

https://doi.org/10.1017/S0263574723000449 Published online by Cambridge University Press

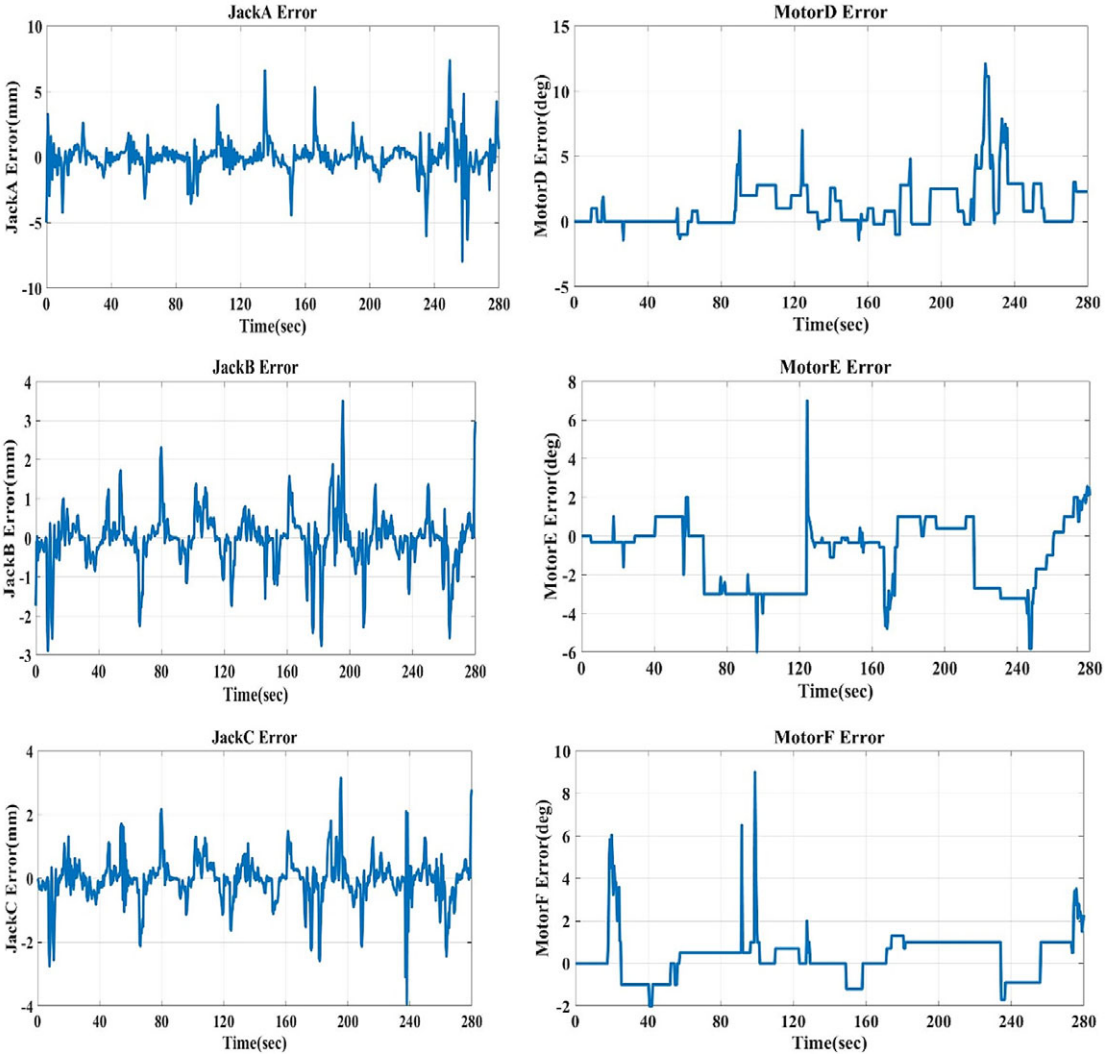

Figure 24. *The error profiles of the main actuators during the climbing procedure.*

This huge change in the robot's altitude and configuration shows the high maneuverability and stability of the robot in the field of the earth's gravity. Thus, it can be concluded that the desired workspace of the robot toward climbing to its desired location can be realized since the desired joint space tracking is fulfilled. Therefore, the designed and manufactured robot is able to ascend through the infrastructures and implement its inspectional or operational task successfully in its desired height level.

6. Conclusion

A novel grip-based climbing robot was designed and manufactured in this paper which is able to ascend through the scaffolds and infrastructures in order to implement inspectional and operational tasks. The designed robot is a hybrid system equipped with a novel gripping mechanism that can tolerate a considerable load and is robust against slippage. It was explained that the locomotion of the robot is inspired by monkeys' movement through the trees, and as a result, the stability of the system is assured since always two limbs are connected to the pipes simultaneously. Moreover, it was stated that the robot's degree of mobility is high enough since the designed mechanism is redundant, and thus, path planning and optimization are possible. The robot has five DOFs moving in the planar workspace

https://doi.org/10.1017/S0263574723000449 Published online by Cambridge University Press

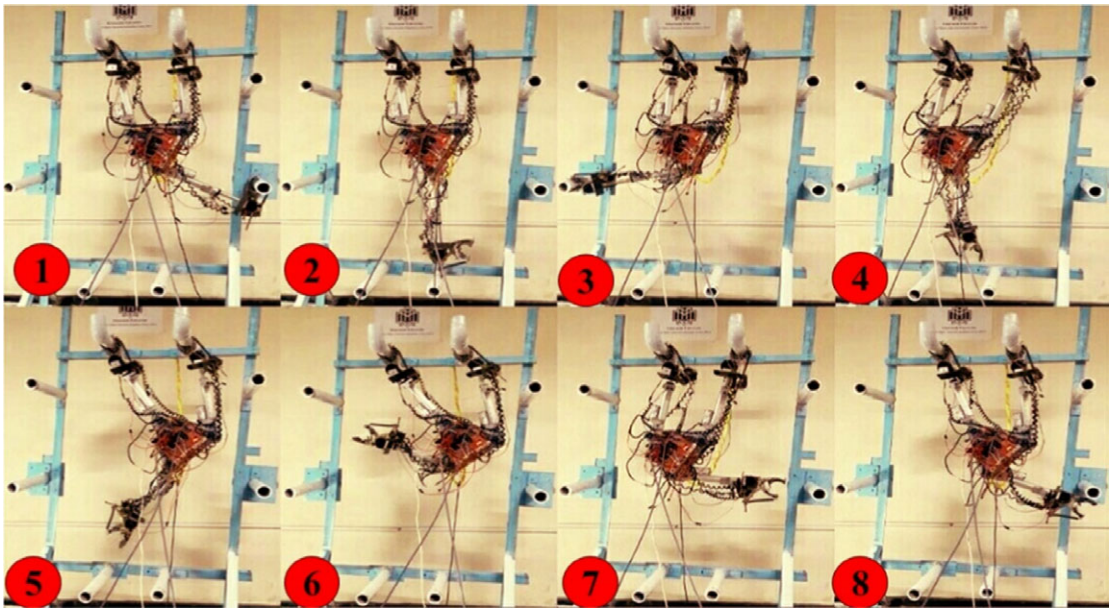

Figure 25. *The maneuverability of the KharazmBot during the manipulation in the desired height.*

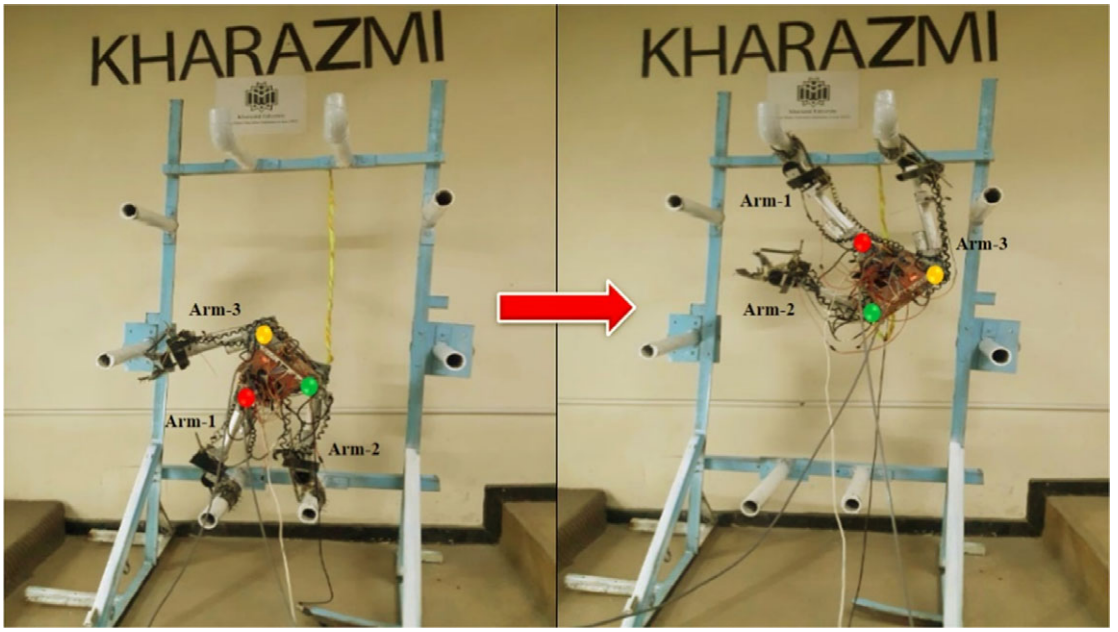

Figure 26. *The initial and final position of the robot after the combination of the climbing and manipulating procedures.*

while its related grippers have one DOFs for gripper orientation and one for open/close operation, respectively. The corresponding model of the robot was then extracted by which the controlling procedure can be accomplished. Afterward, a prototype of the proposed climbing robot (KharazmBot) was manufactured at Kharazmi University, and its related procedure of fabrication was completely explained. All of the mechanical parts are manufactured precisely according to the design demands, and the assembling process was introduced using proper connections and power transmission systems. Required rotational and linear actuators were then selected according to the required kinetic capabilities

https://doi.org/10.1017/S0263574723000449 Published online by Cambridge University Press

of the robot, and the actual movement of the robot was recorded using rotational and linear sensors. A feedback-based controller was designed to realize the desired tracking of the robot implemented by the operator. All of the sending commands and receiving data can be handled with the aid of an Arduino Due microcontroller based on Arm architecture in a real-time way. A general GUI was finally designed for the robot in the LabView environment through which the operator can control the robot graphically in an operating control panel. The ability of the designed robot for ascending through the mentioned structures and also its efficiency in realizing good mobility and stability was investigated by conducting some experimental tests on the manufactured robot. The climbing procedure was first designed and simulated in ADAMS and then was implemented on the manufactured robot of KharazmBot. The ability of the designed robot for climbing through the scaffolds was checked, and the required motors' torques were compared with the allowable torque range of the employed motors with the aid of the mentioned simulation in ADAMS. Comparing the results of experimental tests obtained from the sensors and the data provided by LabView proved the efficiency and accuracy of the robot toward accomplishing the expected mission of climbing. The norm of error between these two profiles is less than 5° for rotary motors and 5 mm for linear jacks which confirms the mentioned verification. Finally, the manipulating ability of the robot at its final stage was shown by another experimental test. Thus, it can be concluded that the designed and manufactured climbing robot of this paper has the ability to carry a special detector or manipulator to the desired height of a high structure and implement the required inspectional or operational task successfully, with good stability and accuracy.

Author contributions. V. Boomeri designed the robot and modeled the robot and simulated it by MATLAB and cooperated in the construction and providing its electrical equipment with robot programming.

H. Tourajizadeh proposed the idea climbing robot through the scaffold, supervised the modeling and simulation of the system, and wrote the manuscript.

H. R. Askarian modeled the robot in SOLIDWORKS, extracted the related drawings, and cooperated in manufacturing and assembling the mechanical parts of the robot.

S. Pourebrahim modeled the robot in MSC-ADAMS and cooperated in manufacturing the robot.

Financial support. The authors would like to thank ***Iran National Science Foundation*** for its financial support to research project No. 96005846.

Conflicts of interest. The authors declare that there is no conflict of interest.

Ethical approval. Not applicable.

References

[1] C. Balaguer, A. Gimenez and A. Jardón, "Climbing robots' mobility for inspection and maintenance of 3D complex environments," *Auton. Robots* **18**(2), 157–169 (2005).

[2] D. Schmidt and K. Berns, "Climbing robots for maintenance and inspections of vertical structures—A survey of design aspects and technologies," *Robot. Auton. Syst.* **61**(12), 1288–1305 (2013).

[3] S. A. Stoeter and N. Papanikolopoulos, "Autonomous stair-climbing with miniature jumping robots," IEEE Trans. Syst. Man. Cybern. B Cybern. 35(2), 313–325 (2005).

[4] A. Bhole, S. H. Turlapati, V. Rajashekhar, J. Dixit, S. V. Shah and K. M. Krishna, "Design of a robust stair-climbing compliant modular robot to tackle overhang on stairs," *Robotica* **37**(3), 428–444 (2019).

[5] J. Resino, A. Jardón, A. Giménez and C. Balaguer, "Analysis of the Direct and Inverse Kinematics of ROMA II Robot," **In:** *Climbing and Walking Robots* (Springer, Berlin/Heidelberg, 2006) pp. 869–874.

[6] H. Zhu, Y. Guan, C. Cai, L. Jiang, X. Zhang and Zhang H., "W-Climbot: A Modular Biped Wall-Climbing Robot," **In:** *2010 IEEE International Conference on Mechatronics and Automation* (IEEE, 2010).

[7] A. Sadeghi, H. Moradi and M. N. Ahmadabadi, "Analysis, simulation, and implementation of a human-inspired pole climbing robot," *Robotica* **30**(2), 279–287 (2012).

[8] J. Liu, L. Xu, S. Chen, H. Xu, G. Cheng and J. Xu, "Development of a bio-inspired wall-climbing robot composed of spine wheels, adhesive belts and eddy suction cup," *Robotica* **39**(1), 3–22 (2021).

[9] R. Aracil, R. Saltarén and O. Reinoso, "Parallel robots for autonomous climbing along tubular structures," *Robot. Auton. Syst.* **42**(2), 125–134 (2003).

[10] F. Xu, S. Dai, Q. Jiang and X. Wang, "Developing a climbing robot for repairing cables of cable-stayed bridges," *Automat. Constr.* **129**, 103807 (2021).

https://doi.org/10.1017/S0263574723000449 Published online by Cambridge University Press

[11] Abderrahim M., Balaguer C., Giménez A., Pastor J. M. and Padron V., "ROMA: A Climbing Robot for Inspection Operations," **In:** *Proceedings 1999 IEEE International Conference on Robotics and Automation* (IEEE, 1999).
[12] Y. Liu, Y. Yu, D. Wang, S. Yang and J. Liu, "Mechatronics design of self-adaptive under-actuated climbing robot for pole climbing and ground moving," *Robotica* **40**(7), 2255–2274 (2022).
[13] M. Tavakoli, L. Marques and A. T. de Almeida, "A low-cost approach for self-calibration of climbing robots," *Robotica* **29**(1), 23–34 (2011).
[14] N. Zhu, H. Zang, B. Liao, H. Qi, Z. Yang, M. Chen, X. Lang and Y. Wang, "A quadruped soft robot for climbing parallel rods," *Robotica* **39**(4), 686–698 (2021).
[15] W. Wang and S. Wu, "A caterpillar climbing robot with spine claws and compliant structural modules," *Robotica* **34**(7), 1553–1565 (2016).
[16] J. Yao, S. Gao, G. Jiang, T. L. Hill, H. Yu and D. Shao, "Screw theory based motion analysis for an inchworm-like climbing robot," *Robotica* **33**(8), 1704–1717 (2015).
[17] Yoon Y. and Rus D., "Shady3d: A Robot that Climbs 3D Trusses," **In:** *Proceedings 2007 IEEE International Conference on Robotics and Automation* (IEEE, 2007).
[18] Y. Guan, L. Jiang, H. Zhu, W. Wu, X. Zhou, H. Zhang and Zhang X., "Climbot: A bio-inspired modular biped climbing robot—system development, climbing gaits, and experiments," *J. Mech. Robot.* **8**(2), 021026 (2016).
[19] P. Biswal and P. K. Mohanty, "Modeling and effective foot force distribution for the legs of a quadruped robot," *Robotica* **39**(8), 1504–1517 (2021).
[20] Bevly D. M., Farritor S. and Dubowsky S., "Action Module Planning and Its Application to an Experimental Climbing Robot. **In:** *2000 Proceedings ICRA'00 IEEE International Conference on Robotics and Automation* (IEEE, 2000).
[21] Li H., Ceccarelli M., Huang Q. and Carbone G., "A Chameleon-Like Service Robot for Space Station," **In:** *International Workshop on Bio-Inspired Robots*, Nantes, France (2011).
[22] Q. M. Marwan, S. C. Chua and L. C. Kwek, "Comprehensive review on reaching and grasping of objects in robotics," *Robotica* **39**(10), 1849–1882 (2021).
[23] M. Honarpardaz, M. Tarkian, J. Ölvander and X. Feng, "Finger design automation for industrial robot grippers: A review," *Robot. Auton. Syst.* **87**, 104–119 (2017).
[24] Hsu J., Yoshida E., Harada K. and Kheddar A., "Self-Locking Underactuated Mechanism for Robotic Gripper," **In:** *2017 IEEE International Conference on Advanced Intelligent Mechatronics (AIM)* (IEEE, 2017).
[25] M. Saliba and C. De Silva, "Quasi-dynamic analysis, design optimization, and evaluation of a two-finger underactuated hand," *Mechatronics* **33**, 93–107 (2016).
[26] P. Vulliez, J.-P. Gazeau, P. Laguillaumie, H. Mnyusiwalla and P. Seguin, "Focus on the mechatronics design of a new dexterous robotic hand for inside hand manipulation," *Robotica* **36**(8), 1206–1224 (2018).
[27] J. E. P. Puig, N. E. N. Rodriguez and M. Ceccarelli, "A methodology for the design of robotic hands with multiple fingers," *Int. J. Adv. Robot. Syst.* **5**(2), 22 (2008).
[28] W. Yan, Z. Deng, J. Chen, H. Nie and J. Zhang, "Precision grasp planning for multi-finger hand to grasp unknown objects," *Robotica* **37**(8), 1415–1437 (2019).
[29] M. Tavakoli, B. Enes, J. Santos, L. Marques and A. T. de Almeida, "Underactuated anthropomorphic hands: Actuation strategies for a better functionality," *Robot. Auton. Syst.* **74**, Part A 267–282 (2015).
[30] M. Modabberifar and M. Spenko, "Development of a gecko-like robotic gripper using Scott-Russell mechanisms," *Robotica* **38**(3), 541–549 (2020).
[31] L. Jiang, Y. Guan, X. Zhou, X. Zhang and H. Zhang, "Grasping Analysis for a Biped Climbing Robot," **In:** *2010 IEEE International Conference on Robotics and Biomimetics* (IEEE, 2010).
[32] F. Xu, F. Meng, Q. Jiang and G. Peng, "Grappling claws for a robot to climb rough wall surfaces: Mechanical design, grasping algorithm, and experiments," *Robot. Auton. Syst.* **128**, 103501 (2020).
[33] S. Andreuchetti, V. M. Oliveira and T. Fukuda, "A survey on brachiation robots: An energy-based review," *Robotica* **39**(9), 1588–1600 (2021).
[34] R. C. Campos, Development of a UAV gripping device for fast coupling, Universidade Federal de Santa Catarina (UFSC) (2021) pp. 29–36.
[35] M. Plooij, G. Mathijssen, P. Cherelle, D. Lefeber and B. Vanderborght, "Lock your robot: A review of locking devices in robotics," *IEEE Robot. Autom. Mag.* **22**(1), 106–117 (2015).
[36] G. Van Oort, R. Carloni, D. J. Borgerink and S. Stramigioli, "An Energy Efficient Knee Locking Mechanism for a Dynamically Walking Robot," **In:** *IEEE International Conference on Robotics and Automation* (IEEE, 2011).
[37] L. L. Howell and A. Midha, "The effects of a compliant workpiece on the input/output characteristics of rigid-link toggle mechanisms," *Mech. Mach. Theory* **30**(6), 801–810 (1995).
[38] V. Boomeri and T. H. Design, "Modeling and manufacturing a new robotic gripper with high load bearing capability and robust control of its mechanical arm," *ADMT J.* **14**(1), 1–17 (2021).
[39] V. Boomeri and H. Tourajizadeh, "Design, modeling, and control of a new manipulating climbing robot through infrastructures using adaptive force control method," *Robotica* **38**(11), 2039–2059 (2020).
[40] Boomeri V., Pourebrahim S. and Tourajizadeh H., "Kinematic and Dynamic Modeling of an Infrastructure Hybrid Climbing Robot," **In:** *2017 IEEE 4th International Conference on Knowledge-Based Engineering and Innovation (KBEI)* (IEEE, 2017).

Cite this article: V. Boomeri, H. Tourajizadeh, H. R. Askarian and S. Pourebrahim (2023). "Design, modeling, and manufacturing of a novel robust gripper-based climbing robot: KharazmBot", Robotica **41**, 2365–2396. https://doi.org/10.1017/S0263574723000449